

A STUDY OF CURRENT SPREAD IN ARTIFICIAL  
ELECTRICAL STIMULATION OF THE COCHLEA

A dissertation submitted in partial fulfillment of the  
requirements for the degree of

MASTER OF TECHNOLOGY

by

GAUTAM. S.K.

Roll No : 883723

Guides

Prof. K.J. Gazder

Dr. P.C. Pandey

School of Biomedical Engineering  
Indian Institute of Technology, Bombay

July 1990

TH-3  
DR PREM PANDEY  
ELECTRICAL ENGG. DEPT.  
I. I. T., POWAI.  
BOMBAY-400 076.

DISSERTATION APPROVAL SHEET

Dissertation entitled "A STUDY OF CURRENT SPREAD IN ARTIFICIAL ELECTRICAL STIMULATION OF THE COCHLEA" submitted by GAUTAM SUDARSHAN KUMAR is approved for the award of the degree MASTER OF TECHNOLOGY in BIOMEDICAL ENGINEERING.

GUIDE

K. S. Srinivasan

CO-GUIDE

P. S. Srinivasan

CHAIRMAN

B. S. Srinivasan

INTERNAL EXAMINER

S. S. Srinivasan

EXTERNAL EXAMINER

R. S. Srinivasan

## ABSTRACT

For the appropriate stimulation of the cochlea in cochlear prosthesis, it is important to study the current spread that takes place within the confines of the cochlea during artificial electrical stimulation. This thesis deals with the study of current spread in tank models as well as scaled-up physical models of scala tympani.

We have measured the potential differences at different distances from an electrode tip submerged in the model, in order to study the current spreading as a function of fluid conductivity, model geometry, stimulation and electrode configuration. The potential differences are seen to fall rapidly when we move away from the electrode in monopolar stimulation.

The data obtained from this study may be useful for stimulus deconvolution techniques in cochlear stimulation strategies.

### ACKNOWLEDGEMENTS

I would like to sincerely thank Prof. K.J. Gazder for his able guidance.

I am highly thankful to Dr. Prem Pandey for his unfailing guidance and encouragement to me throughout the project.

I am also thankful to many of my friends and faculty members interaction with whom helped me to complete the project.

( GAUTAM S.K. )

Abstract

Acknowledgements

## CONTENTS

1.	Introduction	..	1
	1.1. Overview	..	1
	1.2 Project objectives	..	3
	1.3 Outline of the report	..	4
2.	The auditory system	..	6
	2.1 Introduction	..	6
	2.2. Functional anatomy of the cochlea	..	6
	2.3. The auditory pathway	..	13
	2.4 Hearing impairment	..	15

3.	Electrical stimulation for cochlear prosthesis	.. 23
3.1	Introduction	.. 23
3.2	Historical background	.. 23
3.3	Cochlear Prostheses	.. 24
3.3.1	Different stimulation schemes	.. 25
3.3.2	Speech processing schemes	.. 27
3.4	Problems in electrical stimulation of the cochlea..	28
3.5	Multichannel excitation	.. 30
3.6	Current spreading in multichannel excitation	.. 31
4.	Current spread in cochlea	.. 36
4.1	Introduction	.. 36
4.2	Factors affecting current spread	.. 36
4.3	Methods of studying the current distribution	.. 38
4.4	Earlier studies on current spread in the cochlea	.. 39
5.	Study of potential distribution	.. 45
5.1	Introduction	.. 45
5.2	Models for study of potential distribution	.. 45
5.2.1	Tank models	.. 45
5.2.2	Scaled-up physical models of scala tympani	.. 47

5.3	Experimental set-up	.. 49
5.4	Effect of fluid conductivity	.. 52
5.5	Effect of model geometry	.. 53
5.6	Effect of stimulation waveform	.. 54
5.7	Effect of electrode configuration	.. 55
5.8	Study with scaled up physical models of scala tympani	.. 55
6.	Results and analyses	.. 66
6.1	Introduction	.. 66
6.2	Current density from potential distribution	.. 66
6.3	Effect of fluid conductivity	.. 68
6.4	Effect of model geometry	.. 69
6.5	Effect of stimulation waveform	.. 70
6.6	Effect of electrode configuration	.. 71
6.7	Potential distribution in scala tympani models	.. 71
7.	Summary and Conclusions	.. 94
	References	.. 97

CHAPTER 1

INTRODUCTION

1.1 OVERVIEW

The artificial stimulation of the auditory system results in the perception of the sensation of sound. Cochlear prosthesis is a sensory aid for persons with profound sensori-neural hearing loss. The device functions by converting acoustic signals to electrical currents that stimulate the residual auditory nerve fibres by way of electrodes placed in their vicinity (Gray, 1985).

A major problem in this type of artificial electrical stimulation is that stimulation sites are remote from neural tissue resulting in current spreading and less localised stimulation. There is less localised stimulation of the nerve fibers because of the spread of current along the fluid filled spaces of the cochlea and away from the group of nerve fibers to be stimulated.

It is not known how the electric field densities are built up and dissipated within the cochlea (House, 1986). However, the electric fields from different electrodes generally overlap to excite common sub-populations of neurons. So a multielectrode array will not necessarily

produce true multichannel stimulation if the electric fields generated by the electrodes overlap significantly. This overlap in excitation fields is the problem of channel interaction which can severely limit the performance of multichannel prosthesis (Pickett & Levitt, 1980; Black et al, 1981).

For this reason, it becomes necessary to carry out basic electrophysiological studies to determine the best methods of sharpening the current field and restricting it to a localized area (Clark et al, 1978). It may be possible to use the information on the current spreading characteristics to select the stimulation pattern to compensate for it. A 'current deconvolution' scheme for computing the current patterns to be placed on the electrodes, that will result in desired current density distribution at nerve endings may provide one such solution, provided that difficulties pertaining to computational problems and practical limitations relating to the accuracy of current spread measurements could be sorted out (Pandey, 1987)

## 1.2 PROJECT OBJECTIVES.

When the electrodes pass electric currents into the perilymph, the current spreads around the electrodes. The neural tissue nearest the electrode gets maximal stimulation by this stimulus but between two electrodes there is a mix-up of the two different stimuli and overlapping of electric fields of the two electrodes enclosing the area. We would like to look into the problem of how best to utilize current to stimulate the intervening areas to the desired level and also as to what type of stimulus in the nearby electrodes would cause such a stimulation in this intervening area. In other words, if we know the behaviour of current spread, then we could deconvolve, i.e., we could compute out the type of stimulus that is to be given at the electrodes so as to get a certain current stimulus in the intervening areas. With the help of such a deconvolution technique, we should attempt at providing desired stimulation at a larger number of sites with a small number of electrodes. Thereby we would be better utilizing the tonotopic arrangement of the auditory neural fibres along the basilar membrane. Information on the current spread behaviour is important for developing deconvolution techniques.

The object of this project is to study the current spread in scaled-up models of the cochlea. The potential differences at different distances from an electrode tip submerged inside a conducting fluid, will be measured. This is in order to study the current spreading as a function of fluid conductivity, model geometry, stimulation and electrode configuration. This gives us the directly recorded values of the current spread that occurs around the electrodes which will be compared with other studies reported in literature.

### 1.3 OUTLINE OF THE REPORT

Chapters 2, 3 and 4 provide background material. The topics presented in the second chapter include the functional anatomy of the auditory system and perceptive hearing impairment. The history of electrical stimulation of nerve fibres, the cochlear prostheses and problems related with the electrical stimulation of the cochlea are discussed in the third chapter. Fourth chapter discusses the general behaviour of current spread around electrodes submerged in a conducting liquid. The methods of measuring this and the factors that affect the spread behaviour are also dealt in this chapter. The chapter ends with an overview of other related studies reported in the literature especially pertaining to this problem in cochlear prosthesis.

The physical models used, the experimental set up and the experiments for measuring potential distribution are discussed in Chapter 5. Chapter 6 presents the experimental results and their analyses. Summary and conclusions from this study and suggestions for further work are given in Chapter 7.

## CHAPTER 2

### THE AUDITORY SYSTEM

#### 2.1 INTRODUCTION

This chapter provides an overview of auditory pathway and hearing impairment.

#### 2.2 FUNCTIONAL ANATOMY OF THE AUDITORY SYSTEM

The auditory system can be divided into two functional parts : the sound conducting part and the sound perceiving part (Muhamud, 1984). The sound conducting apparatus is formed by the outer and middle ear. The outer ear consists of the pinna and the external auditory canal as shown in Fig 2.1. The middle ear consists of the tympanic cavity with its three ossicles: malleus, incus and stapes and is seperated from the outer ear by the tympanic membrane to which is attached the malleus as shown in Fig 2.2 The stapes footplate is attached to the oval window of the cochlea. The Eustachian tube connects the middle ear to the nasopharynx and functions to equalize the air pressure on both sides of the eardum. The sound perceiving part consists of the inner ear and the central auditory system. The auditory part of the inner ear consists of the cochlea which is a bony spiral

nearly 35 mm in length coiled upon itself for two and three-fourth turns as shown in Fig. 2.3 Its cross sectional area is about 4 sq. mm at the base and about 1 sq. mm at the apex. The cochlea is a system of coiled tubes, with three different tubes coiled side by side: scala vestibuli, scala media and scala tympani. In Fig 2.4 (a transverse section through a turn of the cochlea) the scala vestibuli and scala media are shown to be separated from each other by the vestibular or Reissner's membrane and the scala tympani and scala media separated from each other by the basilar membrane. On the surface of the basilar membrane lies a structure, the organ of Corti, which contains a series of mechanically sensitive hair cells as shown in Fig 2.5. These are receptive end-organs that generate nerve impulses in response to sound vibrations. The two outer chambers are filled with perilymph (similar to the extracellular fluid in ionic composition) and communicate freely with each other at the helicotrema as shown in Fig. 2.8. The scala media contains endolymph (similar to the intracellular fluid in ionic composition):

The sound waves which are incident on the ear hit upon the eardrum & the eardrum vibrations are transmitted by the ossicular chain to the footplate of stapes on the oval window which is a membrane covering an opening to the scala vestibuli (Birrell, 1984). The footplate is connected with the window's edges by a relatively loose annular ligament so that it can move inward and outward with the sound vibrations. Inward movement causes the fluid to move into the scala vestibuli which increases the pressure and causes the round window to bulge outward as shown Fig 2.8. The flow causes a wavelike displacement of the basilar membrane and the associated structures. Each frequency of sound causes a different 'pattern' of vibration in the basilar membrane and this is one of the important means for frequency discrimination.

The basilar membrane consists of fibres that project from the bony centre of the cochlea, the modiolus, towards the outer wall. These fibres are stiff, elastic reedlike and are not fixed at their distal ends and can vibrate at their free ends. The lengths of the basilar fibres increase progressively from the base of the cochlea to the helicotrema, 0.04 mm at the base to 0.5 mm at the helicotrema, a 12-fold increase in length.

(Guyton, 1984). The diameters of the fibres, on the other hand decrease from the base to the helicotrema so that their overall stiffness decreases more than 100-fold. As a result, the stiff and short fibres near the base of the cochlea have a tendency to vibrate at a high frequency, whereas the long, limber fibres near the apex tend to vibrate at a low frequency.

The elastic tension that is built up in the basilar fibres as they bend initiates a wave that 'travels' along the basilar membrane towards the helicotrema. Each wave is relatively weak at the outset but becomes strong when it reaches that portion of the basilar membrane that has a natural resonance frequency equal to the respective sound frequency. At this point, the basilar membrane can vibrate back and forth with such great ease that the energy in the wave is completely dissipated. Consequently, the wave ceases at this point and fails to travel the remaining distance along the basilar membrane. Thus a high frequency sound wave travels only a short distance before it dies out; a medium frequency sound wave travels about halfway and then dies out; and finally, a very low frequency sound wave travels the entire distance along the membrane as shown in Fig 2.9. Since different regions on the

basilar membrane respond maximally to different frequencies, stimuli of different frequencies will activate spatially separate sets of auditory neurons.

The auditory neurons and the corresponding cells in the cochlear nucleus preserve the orderly arrangement of the sensory cells innervated by them along the basilar membrane and it is maintained to a certain extent in the higher processes of the auditory system as well. This arrangement possibly provides a 'place' coding of the frequency, namely, in terms of the place of maximum stimulation along the basilar membrane. The orderly arrangement of the innervating neurons is known as tonotopic arrangement (Bekesy, 1960).

The actual sensory receptors in the organ are the hair cells, about 3.5 thousand inner hair cells (of diameter 12 microns) forming a single row and about 20 thousand outer hair cells (of diameter 8 microns) arranged in about 3 or 4 rows. The bases and sides of the hair cells are enmeshed by a network of cochlear nerve endings. These lead to the spiral ganglion of Corti, which lies in the modiolus of the cochlea. The spiral ganglion in turn sends axons into the cochlear nerve and thence into the central nervous system.

The minute hairs, or cilia, project upward from the hair cells and are embedded in the surface gel coating of the tectorial membrane, which lies above the cilia in the scala media. Bending of the hair excites the hair cells, and this in turn excites the nerve fibers enmeshing their bases as shown in Fig 2.6.

The upper ends of the hair cells are fixed tightly in a structure called the reticular lamina. The reticular lamina is very rigid and is continuous with a rigid triangular structure called the rods of Corti that rests on the basilar fibers. Therefore, the basilar fibre, the rods of Corti and the reticular lamina all move as a unit. The inward and outward motion of the reticular lamina causes the hairs to sheer back and forth in the tectorial membrane, thus exciting the cochlear nerve fibers whenever the basilar membrane vibrates. Back and forth bending of the hairs causes alternate changes in the electrical potential across the hair cell membrane. This alternating potential is the receptor potential of the hair cell which in turn stimulates the cochlear nerve endings that terminate on the hair cells. The hair cells receive their individual inputs according to a place/time/amplitude distribution that is unique for any type of signal and is due to the travelling waves.

Cochlear nerve fibers, even in the absence of any input, fire spontaneously in a random manner from zero to almost 100/s (Kiang et al, 1972). The random firing represents a noise which limits the detections of signals by the 'read-out' station, the cochlear nuclei. The random firing is partially suppressed by evoked activity and it is one of the reasons why cochlear nerve fibers do not respond to a signal in a deterministic manner.

Each cochlear nerve fibre responds only to a limited range of frequencies. At near-threshold intensities responses are quite narrowly restricted around a frequency known as the best or characteristic frequency of that fibre. The place is also the main determinant of the latency, i.e., the time delay with which a given fibre responds to an acoustic input. The tonotopic relation with respect to both place and time that is caused by the cochlear travelling wave mechanism is maintained throughout the entire auditory system, upto, and including cortical levels.

### 2.3 THE AUDITORY PATHWAY

The nerve fibers from the spiral ganglion form the cochlear nerve as shown in Fig 2.7. These fibers enter the cochlear nuclei located in the upper part of the medulla. At this point, all fibers synapse, and the second order neurons pass mainly to the opposite side of the brain stem through the trapezoid body to the superior olivary nucleus (Chatterjee, 1956). From here they pass up through the lateral lemniscus, and many fibers terminate in the nucleus of the lateral lemniscus but many bypass this nucleus and pass on to the inferior colliculus where most terminate. From here the auditory pathway passes through the peduncle of the inferior colliculus to the medial geniculate nucleus, where all the fibers synapse. From here the auditory tract spreads by way of the auditory radiation to the auditory cortex located mainly in the superior temporal gyrus. Impulses from either ear are transmitted through the auditory pathways of both sides of the brain stem. Crossing over occurs between the two pathways in at least three places. Many collaterals from the auditory tracts pass directly into the reticular activating system of the brain stem and project diffusely up into the cortex and down into the spinal cord. Several important pathways exist from the auditory system to cerebellum which activate the

cerebellar vermis instantaneously in the event of sudden noise. There is a system of efferent fibers that acts as a feedback control both on the hair cells and on their nerve endings.

One feature of the auditory transmission through the cochlear nuclei is the spatial orientation of the pathways for sounds of different frequencies. In the dorsal cochlear nucleus, high frequencies are represented along the medial edge while low frequencies are along the lateral edge. Auditory cortex lies principally on the supratemporal plane of the superior temporal gyrus and adjoining areas of the temporal lobe. Two separate areas, the primary cortex and auditory association cortex are present. The primary cortex is directly excited by projections from the medial geniculate body, while the association areas are usually excited secondarily by impulses from the primary auditory cortex. In the auditory tracts the firing rate is no longer synchronized either with the sound frequency or with that of the cochlear nerve. These findings demonstrate that the sound signals are not transmitted unchanged directly from the ear to the higher levels of the brain (Guyton, 1984). Also the basilar membrane near the base of the cochlea is stimulated by all frequency sounds but by the time the

excitation has reached the cerebral cortex, each neuron responds to only a narrow range of frequencies rather than to a broad range. Somewhere along the path, processing mechanism 'sharpen' the frequency response. Bekesy (1960) hypothesized that this is caused mainly by the phenomenon of lateral inhibition. The auditory cortex is important in the discrimination of tonal patterns.

## 2.5 HEARING IMPAIRMENT

Hearing impairment can be broadly classified into two broad groups. Conductive hearing impairment is associated with the pathology of the sound conducting apparatus, i.e., external or middle ear. Perceptive hearing impairment associated with the pathology of the sound perceiving neurosensory apparatus, i.e., inner ear or any part of the more central mechanism. Perceptive hearing impairment may be classified into four types: sensory, neural, brainstem, and central (Brackman, 1986).

Sensory hearing loss occurs when the sensory elements of the cochlea, i.e., hair cells are diseased so that they are incapable of stimulating the auditory nerve. Neural hearing impairment occurs when the auditory nerve is diseased so that it is incapable of conducting the impulses generated

by the hair cells to the central nervous system. When brain stem structures are incapable of relaying impulses from the auditory nerve to the cortex, a brain stem loss is present. A central hearing loss occurs when the auditory cortex is incapable of making meaningful interpretation of the electrical impulses received from an intact mechanism upto the brain stem.

Most diseases which destroy the auditory nerve also destroy the hair cells so that an isolated neural loss is quite rare and a combined sensory and neural loss fairly common, the so-called sensorineural deafness. Temporal bone studies have shown that even with severe loss of sensory elements, some neurons may still be present. Therefore sensory loss is the most commonly encountered pathology. It is estimated that two thirds of the group of patients with sensorineural hearing impairment are mainly sensory. A brainstem loss is probably uncommon and an isolated central deficit with a normal peripheral mechanism is very rare.

Theoretically it is possible to determine the site of defect in the inner ear and centrally by the measurement of the electrical potentials generated from each of these sites as shown in Fig. 2.10. It is possible to measure the cochlear microphonic from the hair cells, the auditory nerve action potential from the auditory,

the potentials generated in the brain stem and finally the potentials from the auditory cortex with the help of procedures like the electrocochleography, brain stem audiometry and the evoked cortical audiometry respectively. The first site from which a potential is not obtained would be the site of the defect (Brackmann, 1986). The production of each subsequent potential is dependent on the presence of an adequate potential proceeding it. Thus when the hair cells are non-functional, no potentials are produced in the auditory nerve or more centrally even if these structures are intact. Therefore when the cochlear microphonic is absent, another test is resorted to. This test involves electrically stimulating the patient's inner ear through the same needle that we previously used for recording the cochlear microphonic. A low frequency (30 to 120 Hz), low voltage (0.3 to 1.2 V) a.c. stimulation is applied. This current applies an artificial cochlear microphonic to stimulate remaining neural elements. The amplitude of the brain stem responses grows with increasing stimulus intensity. This supplies information of a quantitative nature regarding surviving neuronal population. If the patient perceives sound, this demonstrates that his auditory nerve and more central mechanism is intact and can be classified as an isolated sensory loss. If there is no response to electrical stimulation this indicates a combined neural or more central impairment.

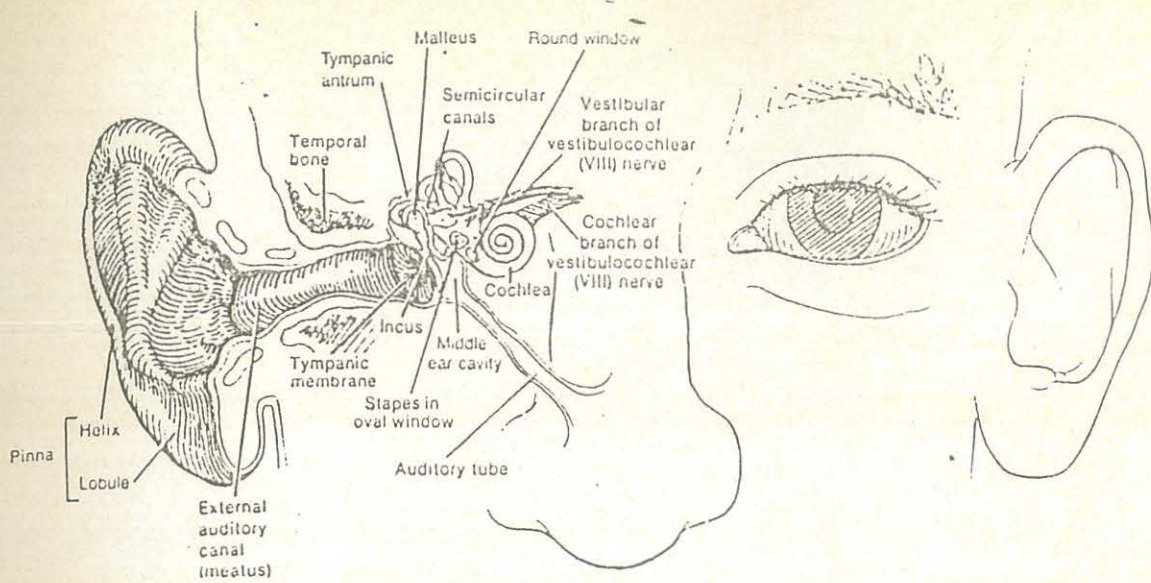


Fig.2.1 The outer, middle & inner ear. The auditory tube is seen connecting middle ear with the nasopharynx.  
Source: Tortora & Anagnostakos (1988) Fig. 17.1.

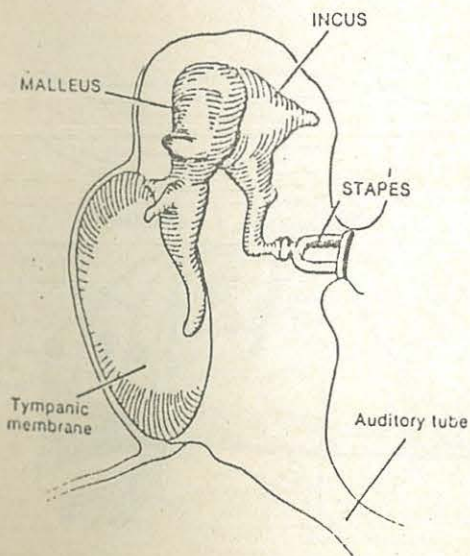


Fig.2.2 The middle ear cavity.  
Source: Tortora & Anagnostakos (1988) Fig. 17.3.

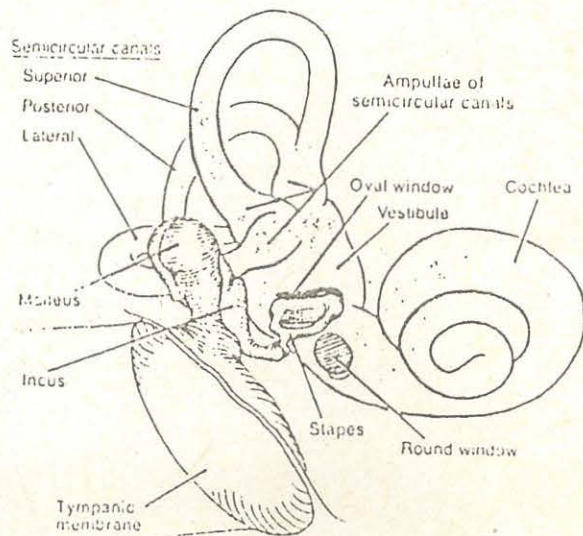


Fig 2.3 Middle & inner ear. Stapes is seen covering the oval window. Round window is also seen.  
Source: Tortora & Anagnostakos (1988) Fig. 17.4

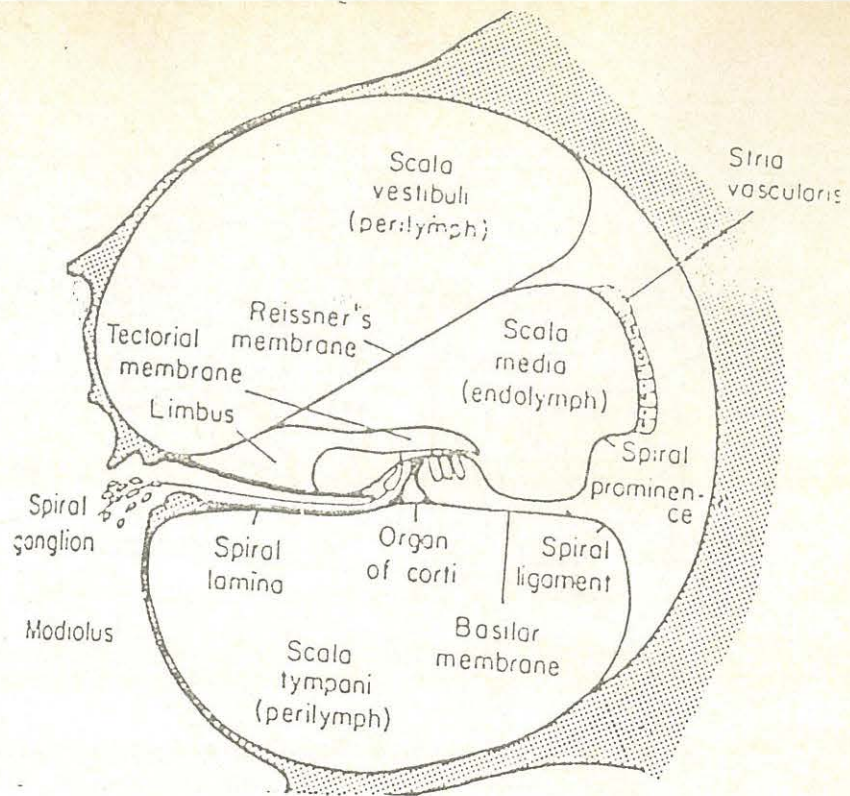


Fig.2.4. A transverse section through a turn of the cochlea  
Source: Pandey (1987) Fig.2.5.

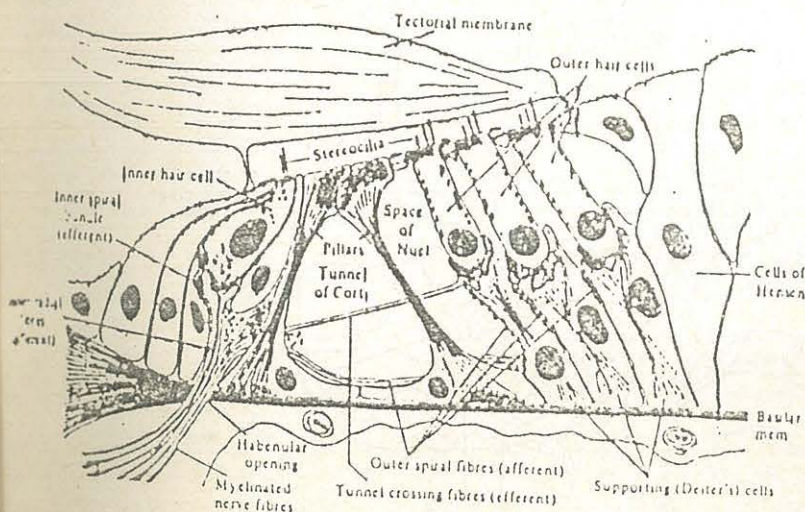


Fig.2.5. A transverse section through organ of Corti  
Source: Guyton (1984) Fig.61.7.

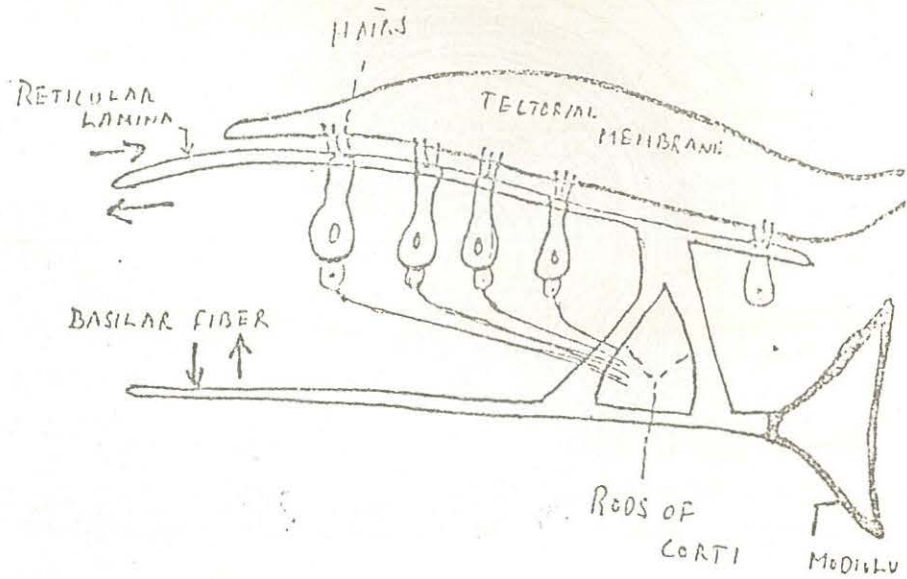


Fig.2.6. Stimulation of the hair cells by to-and-fro movement of the hairs in the tectorial membrane.  
Source: Guyton (1984) Fig.61.8.

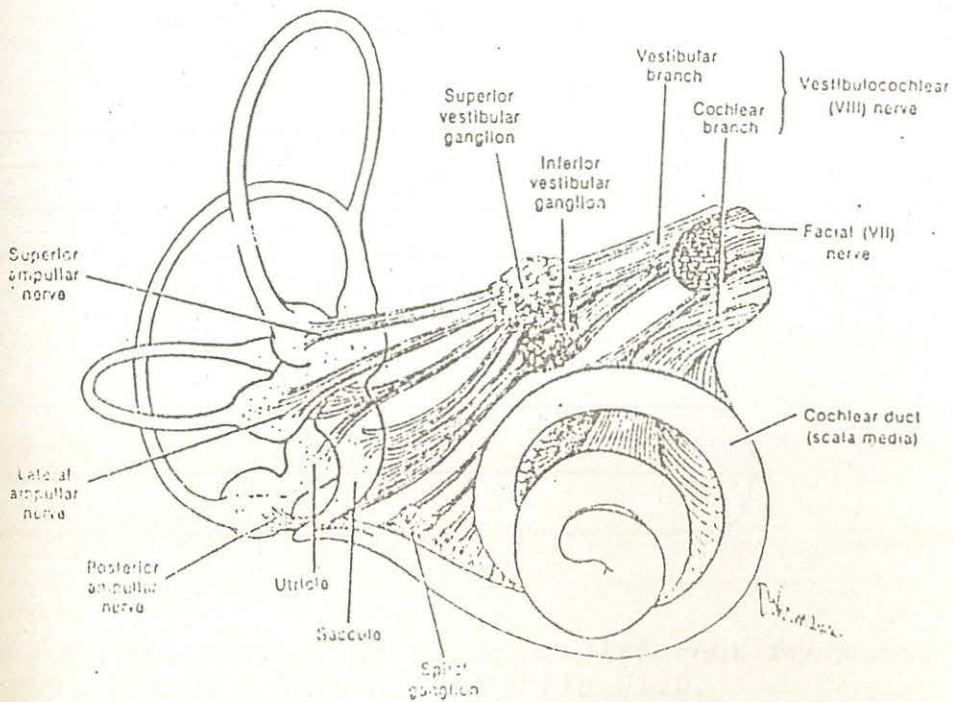


Fig.2.7. Membranous labyrinth and nerves.  
Source: Tortora & Anagnostakos (1988) Fig. 17.8

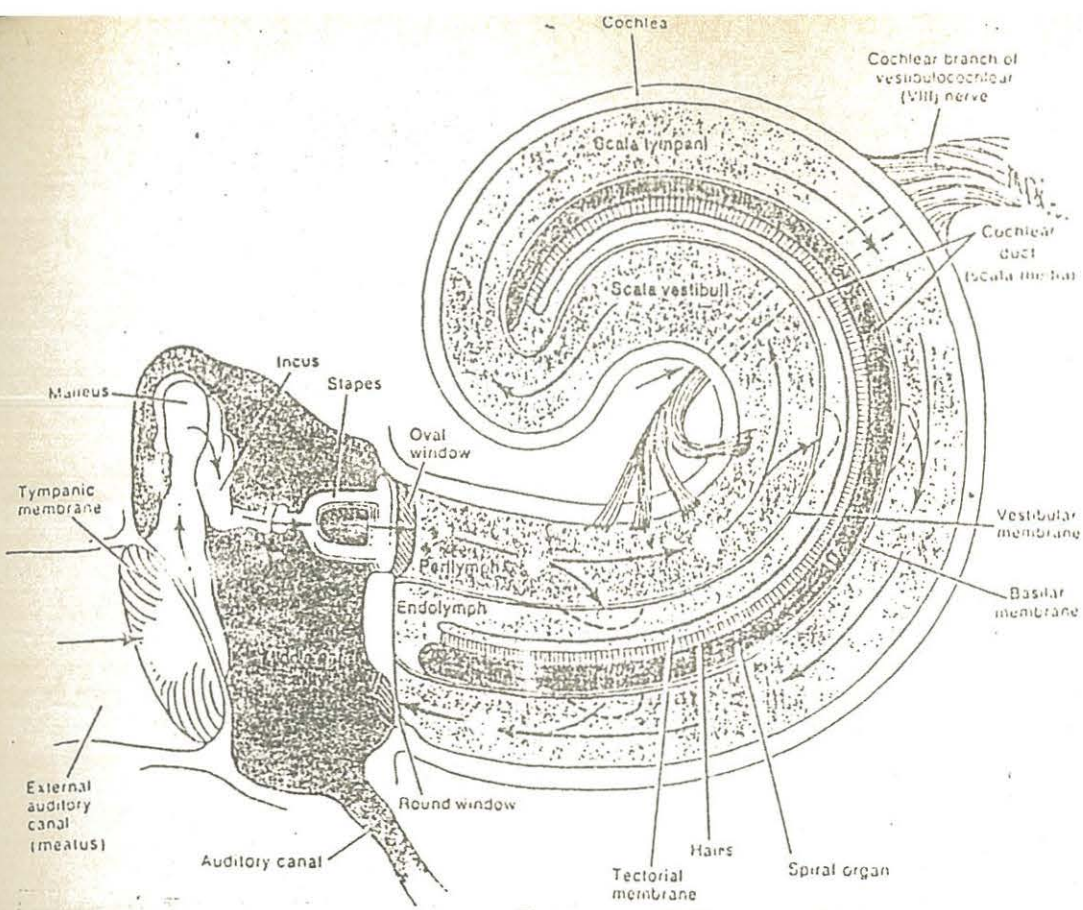


Fig.2.8. The 'travelling wave'.  
 Source: Tortora & Anagnostakos (1988) Fig 17.9

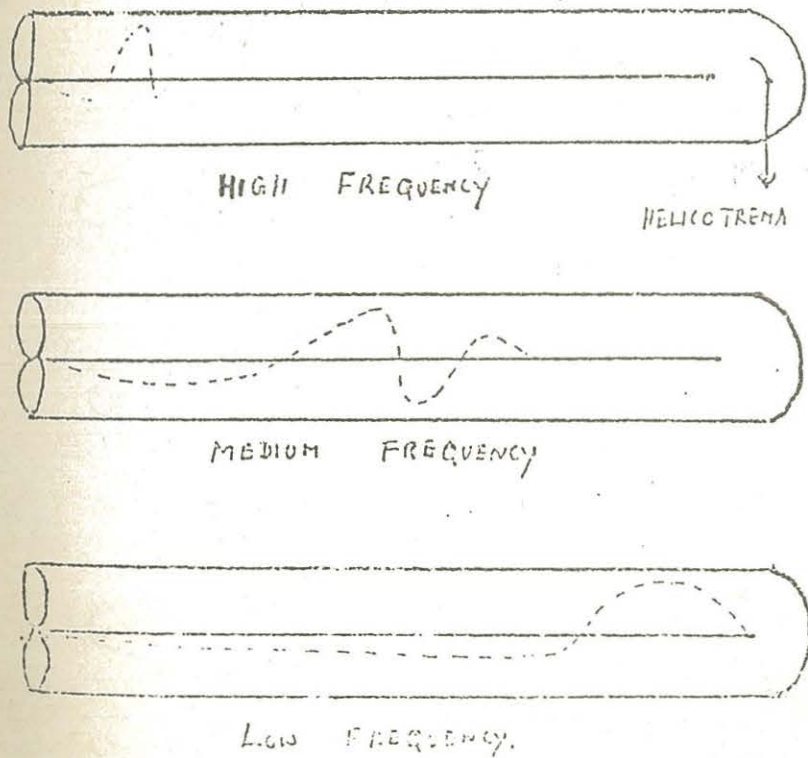


Fig.2.9. The travelling waves of different frequency sounds. Source : Guyton (1984) Fig 61.5.

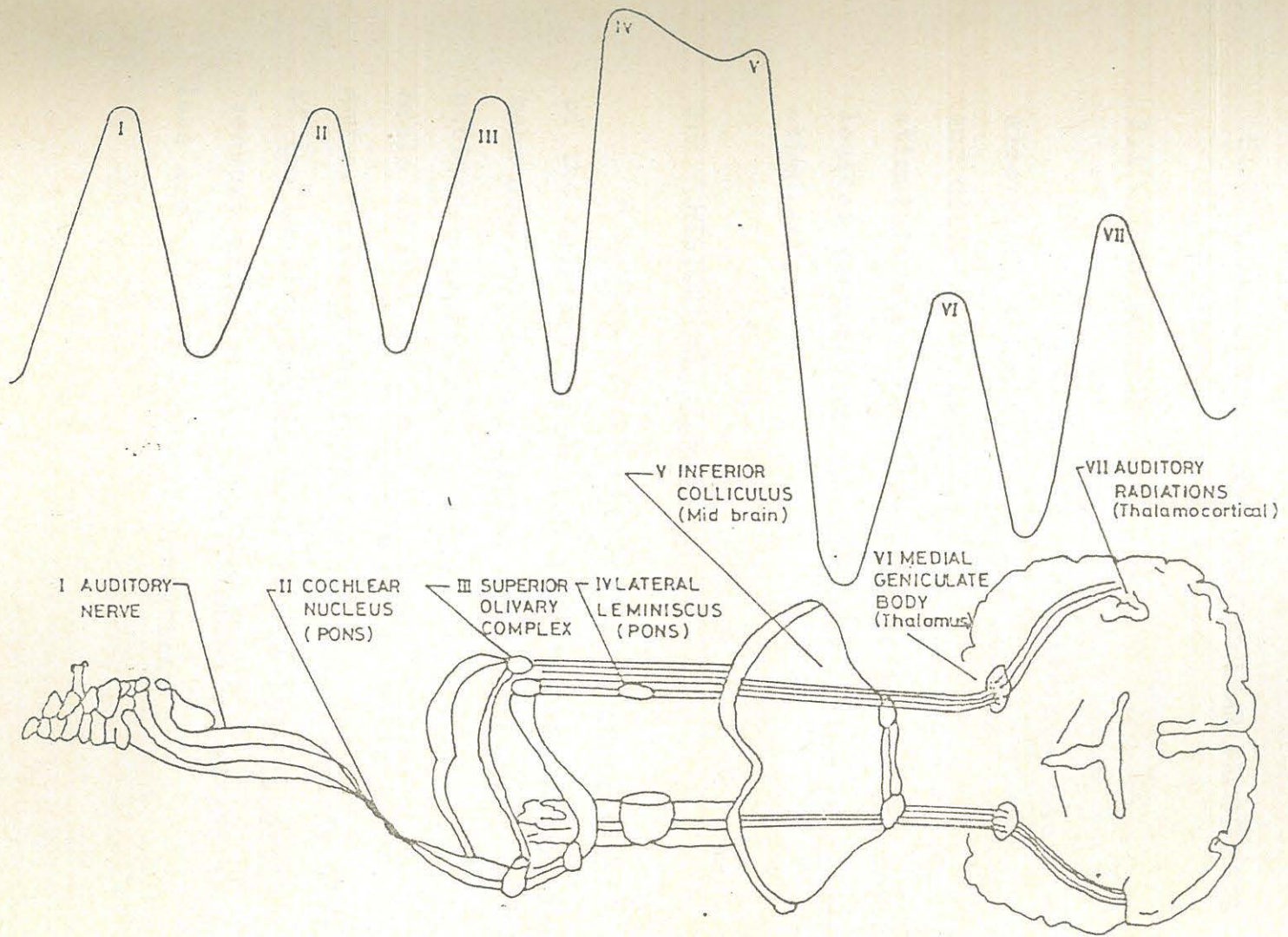


Fig.2.10. The Auditory pathway & waves on evoked response auditory. Source: Audiology department, Ali Yavar Jung Institute of Hearing Handicapped, Bombay.

## CHAPTER 3

## ELECTRICAL STIMULATION FOR COCHLEAR PROSTHESIS

## 3.1 INTRODUCTION

This chapter provides a historical overview of electrical stimulation of the auditory nerve and deals with the problem of appropriate electrical stimulation for cochlear prosthesis and the physiological response of the auditory system to electrical stimulation.

## 3.2 HISTORICAL BACKGROUND

A review of the history of electrical stimulation of the auditory system for evoking hearing percepts has been done by Simmons (1964) and Gray (1985). The first published report of electrical stimulation of human brain is that of a surgeon, Bartholow in 1874. In 1934, Andreef et al published their work 'Electrical stimulation of the hearing organ'. Foerster in 1936 reported that "sensory effects evoked by stimulation of the temporal lobe are chiefly acoustic sensations".

In 1957, Djurno and Eyries reported the first 'cochlear implant'. They inserted a single copper wire inside the cochlea of a 50 year old man who was totally deaf. The electrode was attached to an induction coil placed under skin and indifferent electrode was placed in the temporalis muscle. A number of animal studies were undertaken by Michelson et al in 1968 and these showed that intracochlear electrodes could be maintained safely in cats and would function over long periods of time. Since then a great number of auditory prostheses employing electrical stimulation have been reported (Simmons, 1964; Clark et al, 1978; Keidel & Finkenzeller, 1984; House, 1986).

### 3.3 COCHLEAR PROSTHESES

The basic elements of a typical cochlear prosthesis or implant are shown in Fig 3.1. A microphone picks up acoustic stimuli, converts it into an electrical signal and sends it to the speech processor. The speech processor encodes the signal and this is sent to the transmitting coil which transmits the signal across the skin to the internal coil by magnetic coupling. The internal coil receives and relays the signal to the electrodes which interface with the auditory nerve endings.

The major difference among the different types of implants is in the way in which the resultant electric signal is presented to the stimulating electrode(s), and the type of processing of the incoming signal.

### 3.3.1 DIFFERENT STIMULATION SCHEMES:

Depending on the way the electrical stimulation is presented to the electrode(s), we have single and multichannel types of cochlear implants. In single channel type of implants there is either a single electrode or all the electrodes are activated as one unit. Multichannel implants use the electrode array in one of the several possible configurations for presenting more than one channels of information.

The method of stimulation can be monopolar, bipolar or multipolar, depending on the electrode configuration. In monopolar type of stimulation, the return electrode is placed away from the active electrode. In bipolar configuration, the nearby electrodes act as one pair. In multipolar configuration, some electrodes are used as independent stimulation sites and the rest are connected together as the return electrode.

Depending upon where the interface to the auditory nerve is achieved, cochlear implants can be classified as modiolar, extracochlear, and intracochlear. In modiolar type of implants, the electrodes are directly implanted to the nerve as it exits the modiolum of the cochlea. This has the advantage of providing localised low threshold neural stimulation (Simmons, 1964). However, the exact positions of the electrodes in the nerve with respect to the tonotopic map of the cochlea can not be known and the surgical procedure is difficult. In the extracochlear type of implants, the electrodes are placed outside the cochlea, usually on the round window. This involves less invasive surgery and has less risk of infection and degeneration of inner ear structures. But in this case the stimulation is not localised and there is a possibility of stimulating neural structures other than the auditory nerve. The threshold of extracochlear stimulation is higher. In the intracochlear type of cochlear implants the electrodes are inserted into the scala tympani along the basilar membrane through the round window. This is a relatively simpler surgical procedure and has the advantage of known position of the stimulation sites with respect to the cochlear tonotopic organization (Pandey, 1987).

### 3.3.2 SPEECH PROCESSING SCHEMES

Speech is a complex acoustic signal and considerable processing and encoding is required before it can be presented to the residual auditory nerve fibers, bypassing the hair cells. Four general encoding strategies can be identified in the present day cochlear implants (Fravel, 1986): the neurophysiological approach, the feature extraction approach, the analog approach, and the psychophysical approach.

The neurophysiological based approach attempts to encode acoustic signals the way they are thought to be encoded by the transducer-hair cells in a normal cochlea. This seeks to replace the function of the normal cochlea and tries to duplicate the place code used by a normal auditory system. The feature extraction approach extracts from the auditory environment certain features that are thought to be most important for perception and discards the rest. The analog approach, on the other hand, aims to present as much information as possible to the auditory nervous system by presenting the electrical analog of the acoustic signal. The psychophysical approach takes the maximum advantage of the capacities and transfer characteristics of the system. The capacity of the electrically stimulated auditory nervous system to handle

various aspects of electrical stimulation and the transfer characteristics for electrical stimuli are determined by psychophysical testing.

#### 3.4 PROBLEMS IN ELECTRICAL STIMULATION OF THE COCHLEA

The specificity of nerve fibers for transmitting only one type of sensation, regardless of what type of stimulus excites the fiber, is called the 'labeled line' principle (Guyton, 1984). This property of the nerve fibers is taken advantage of in electrically stimulating the cochlear nerve fibers to perceive sound sensation. The cochlear nerve fibers can be stimulated by small electric currents of the order of a few microamperes. The excitation of a given fibre placed in the field depends on the current density at its location, the conductivity of the medium and on the signal duration. To maximize the desired effect, i.e., to keep the stimulating current as low as possible and to minimize the undesirable effects such as stimulating other unwanted fibers or damaging tissues by generating large stray currents, it is necessary to bring the electrode as close as possible to the fiber to be stimulated.

Tissue fluids can be considered to be electrolytes of 150 millimole/litre sodium chloride. Therefore there is the problem of electrolysis and polarisation when electrodes pass electrical currents into them. The problem of heavy metals ions and their salts causing toxicity to biologic tissues is overcome by the use of noble metals which do not ionize easily such as certain alloys made of 10% iridium and 90% platinum and by the use of 'non-polarizable' electrodes. Metals may also be protectively coated by say carbon (Tonndorf, 1986).

There is very little space in the scala tympani; its average cross-section being about 1 sq mm (Muhamud, 1984). The finest diameter in which platinum wire is commercially available is 8 micrometers. If drawn out thinner, the material loses all its structural strength. The insulating material (teflon), around the wire will make it stiffer, but will increase the diameter to at least three times that of the uninsulated wire. Therefore there is a limit to the number of electrodes that can be introduced via the round window without unduely cramming and dislocating the scala media. One solution for this is to use thin-film techniques, i.e. conducting metal films deposited on plastic, teflon or mylar.

### 3.5 MULTICHANNEL EXCITATION

Discrete segments of the array must be independently controlled to use the tonotopic organization of peripheral neurons and their central processes. To optimize the specificity of these stimulation foci, animal studies, computer models and psychophysical results from patients are used to compare the electric fields of stimulation produced by several different orientations of electrode contacts. A current of 20 A may activate neurons and/or fibers within several hundred microns of the electrode (Tonndorf, 1986), but may be selective as to which neural elements are stimulated. Also there may be multiple auditory pathways diverging from the locus of stimulation. The stimulated neurons may not feed into all of the ascending paths, or if all paths are activated, the pattern of activation may not be similar to naturally occurring patterns of activity.

There are certain differences in the response of the auditory system to acoustic stimulation and that to electrical stimuli (Pandey, 1987). For acoustic stimuli, the nerve fibers usually have a response dynamic range of 20-25 dB. For electrical stimulation this range is only 2-15 dB. The cochlear nerve fibers have almost no

intrinsic frequency selectivity to electrical stimulation but are broadly tuned showing no frequency discrimination compatible with the place principle. For electrical stimulation frequencies below 300-500 Hz, frequency changes can be detected and are reported to be like changes in the pitch. However, the ability to detect frequency changes is much lower than that for normal hearing : the smallest detectable change in the frequency for electrical stimulation frequencies between 100 and 200 Hz is typically 5-30 percent, whereas the same for normal hearing is about 1 percent.

### 3.6 CURRENT SPREADING IN MULTICHANNEL EXCITATION

There is the problem of current spreading and overlapping of the adjacent electric fields. It is difficult to determine as to how many groups of nerve fibers should be stimulated and how well can the electrical stimulus current be restricted to each group. Newer multichannel scala tympani implants are designed to orient the electrodes close to the fibers and to narrowly restrict currents within the vicinity of each channel. Other techniques for limiting current spread and maximizing channel separation involve placing return electrodes on either side of the stimulating electrode or arranging the stimulation pattern so that current spread beyond the

desired region are cancelled by currents on surrounding electrodes. For this, knowledge of the current spread behaviour is essential.

Transmitter coil  
from Speech processor

Receiver coil & stimulator

Round window

[ Cochlear NERVE

Implant electrodes

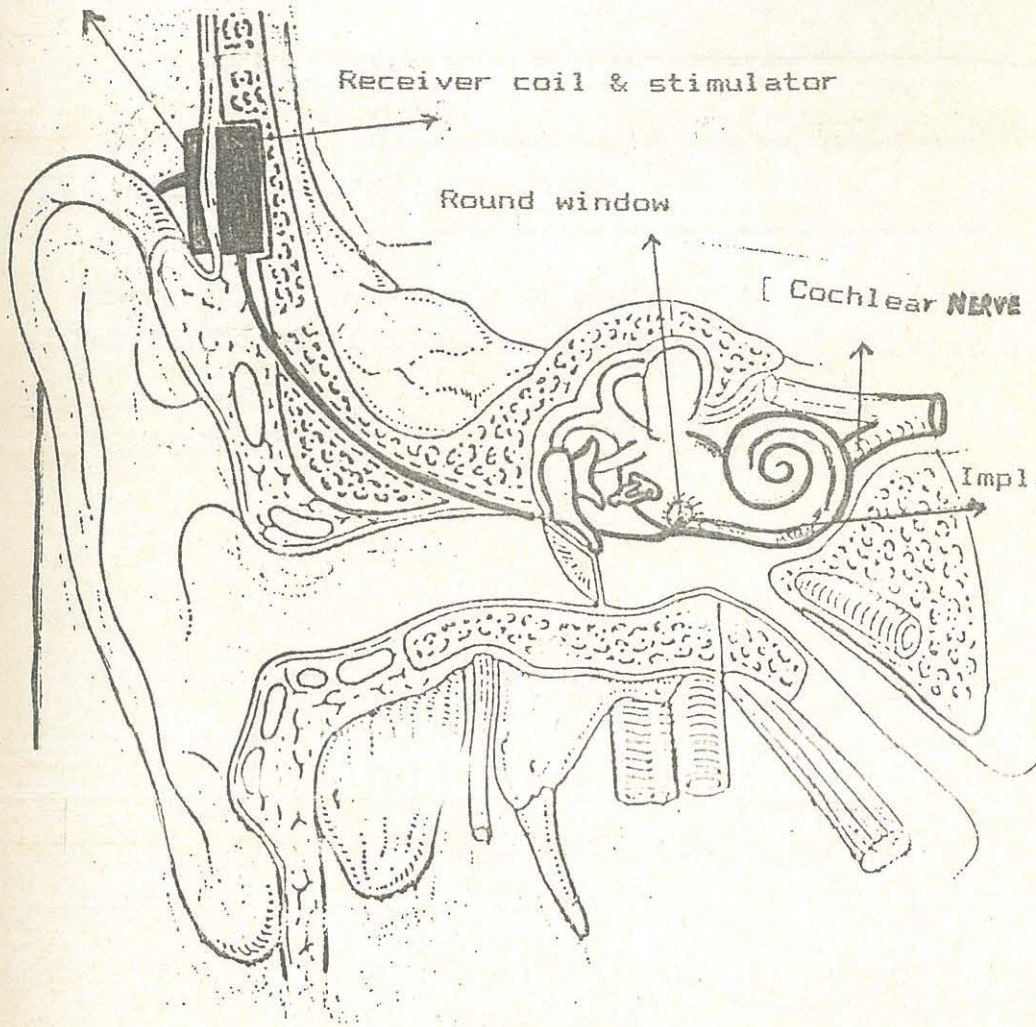


Fig 3.1. Cochlear Implant  
Source; Brackmann (1988) Fig.6.12.

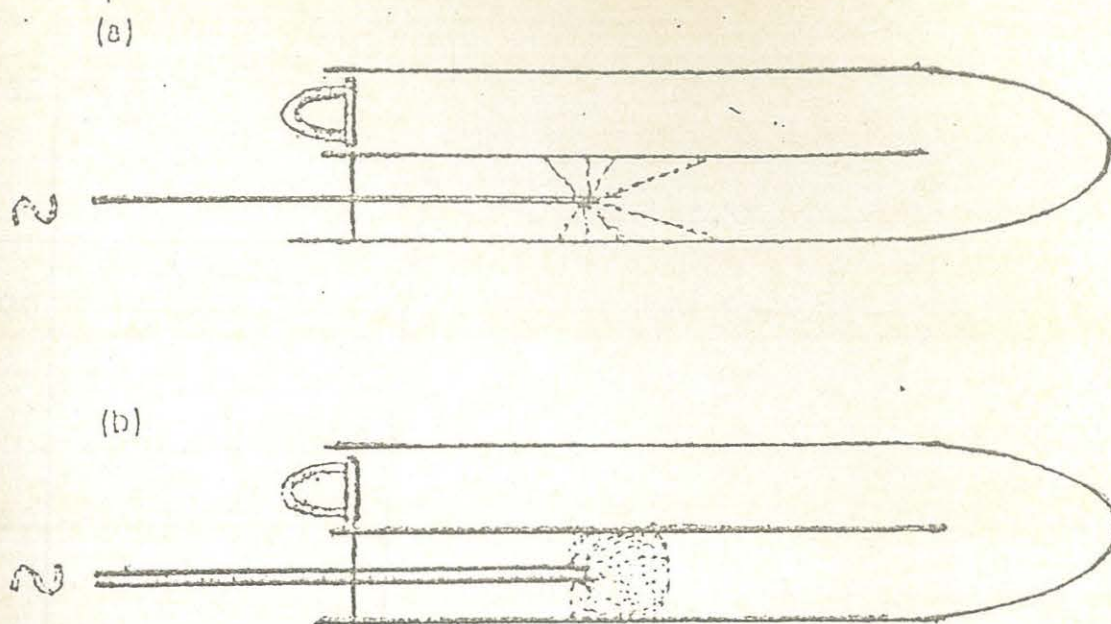


Fig.3.2. Current pathways between electrodes.  
 Source: Tonndorf(1986) a) Monopolar b) Bipolar electrodes.

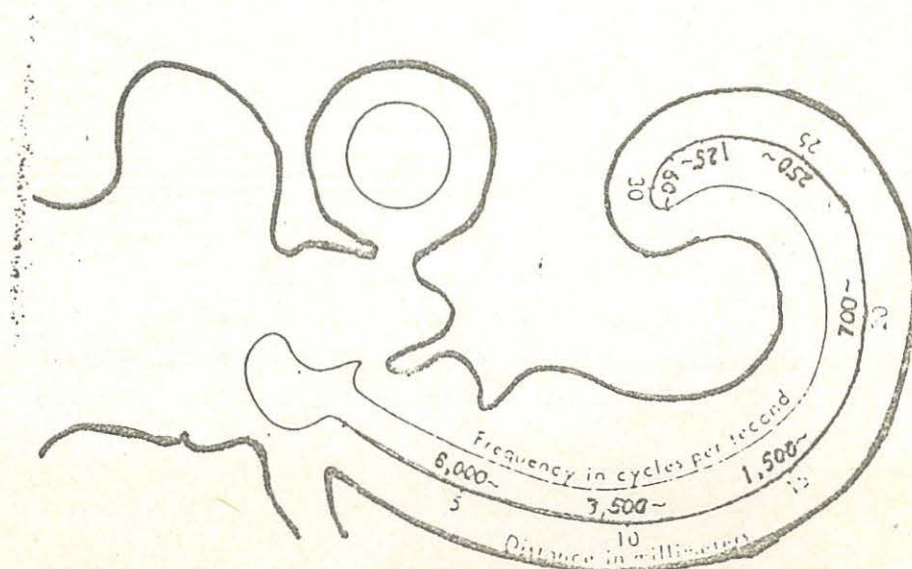


Fig.3.3. Frequency location along the basilar membrane.  
 Source: Zemlin (1985).

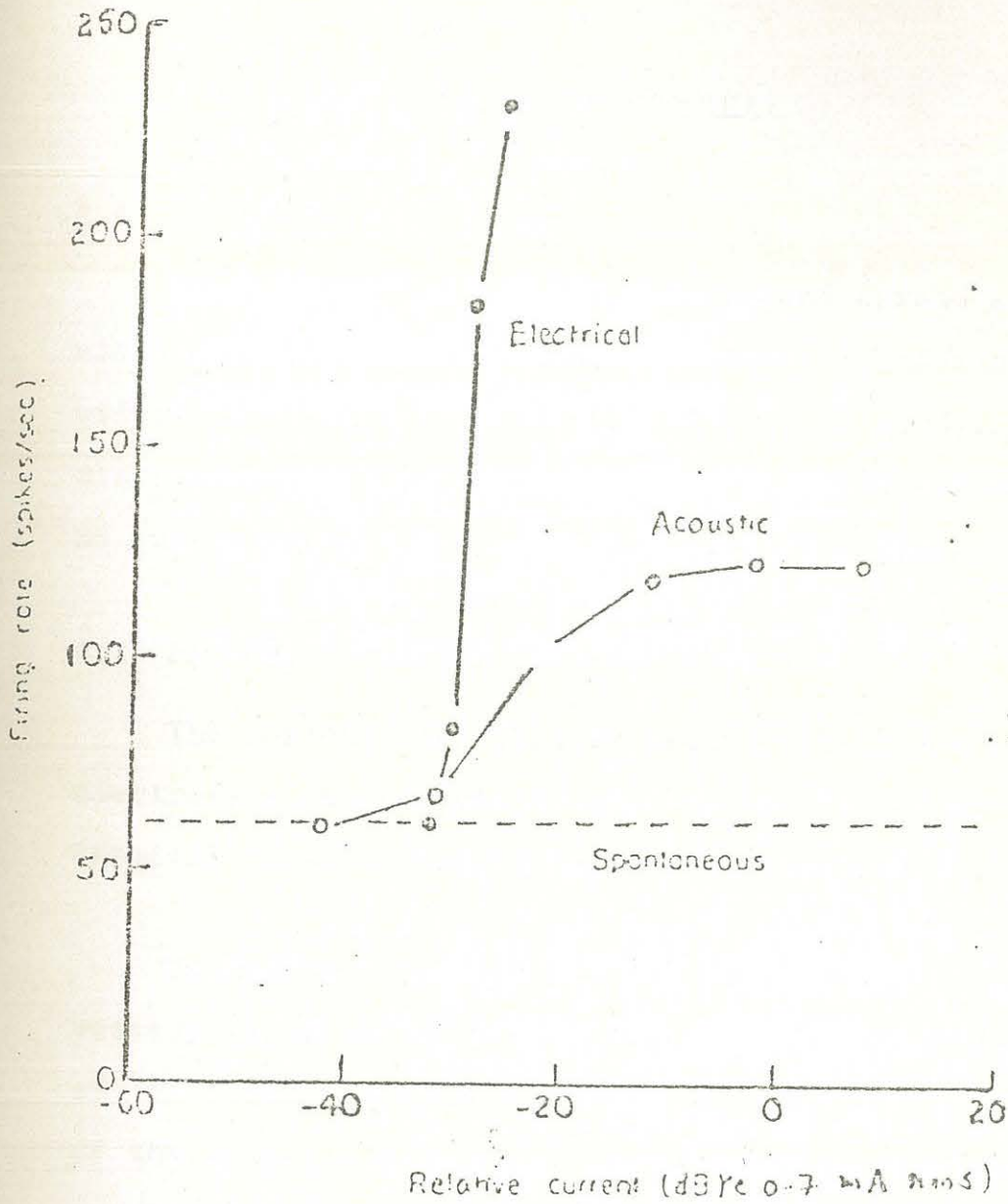


Fig.3.4. Rate-Intensity functions of the auditory nerve fibers for acoustic stimuli and electric stimuli. Source: Kiang & Moxon (1972)

## CHAPTER 4

## CURRENT SPREAD IN COCHLEA

## 4.1 INTRODUCTION

This chapter deals with the current spread around electrodes submerged in an electrolyte, the factors which affect this behaviour, and the methods of studying current distribution. This is followed by a review of the literature on current spread as related to cochlear implants.

## 4.2 FACTORS AFFECTING CURRENT SPREAD

The current distribution around electrodes in an electrolyte depends mainly on geometrical and electrochemical factors (Vagramyan & Solov'ena, 1961).

Geometrical factors are the shape and size of the vessel, shape and size of the electrodes, the position of the electrodes relative to each other and to the walls of the vessel. Electrical and electrochemical factors are the polarization, the electrical conductivity of the solution, factors which influence these values like current density, composition and temperature of the electrolyte, viscosity, and pH etc. Then there are some other factors such as the nature of the electrode metal, the condition of its surface, its heterogeneity in regard to both composition and structure, etc.

It is known that when a certain potential difference is applied to the electrodes, the value of the current passing through the electrolyte will be determined by the total resistance of the system. This resistance has three components (i) the contact resistance  $R_c$  which arises at the electrode/solution interface, (ii) the resistance  $R_e$  of the electrolyte, and (iii) the resistance  $R_m$  of the metal electrodes, which is usually very small by comparison with others and may be neglected.

When the contact resistance due to polarization is practically non-existent, the resulting distribution of the current is called the "primary current distribution". This obeys a general relationship known as Laplace's equation and analytical and numerical methods can be used to solve the equation (Pickett, 1979). When, on the other hand, the contact resistance is of the same order as the resistance of the electrolyte, the resulting modified current distribution (that occurs with active polarization) is referred to as the "secondary current distribution".

#### 4.3 METHODS FOR STUDYING THE CURRENT DISTRIBUTION

Methods of studying current distribution on the surface of an electrode can be divided into three main groups:

1. Graphical methods based on the study of the polarization of electrodes.
2. Methods of studying directly the distribution of the current on the surface of the electrode.
3. Methods involving the plotting of the electrical field.

The drawbacks of the graphical method are connected with the difficulty of recording reproducible polarization curves due to unstable nature of polarization. The method involving studying directly the distribution is more useful in studying the metal deposition as in electroplating. The main advantage of the method of plotting of the electrical field is the clarity of the results: the electric field gives a clear picture of the distribution of the current (Vagramyan & Solov'ena, 1961). This method is most useful for our purposes since we would be using alternating current in our experiments as is done in the electrical stimulation of the cochlea which involves little or no polarization effects.

In the method of plotting the electrical field, the two electrodes are rigidly fixed and the differences in potential between different points in the solution are measured. To increase the accuracy of the measurements a sheet of millimetre graph paper is placed under the transparent vessel holding the electrolyte. The values are then plotted by connecting the points with equal potentials, and thereby the so-called equipotential lines are obtained. The lines of force are obtained by drawing lines perpendicular to the equipotential lines. The current density is given by the closeness of the lines of force per unit area of the electrode.

#### 4.4 EARLIER STUDIES ON CURRENT SPREAD IN THE COCHLEA

Lukies et al (1987) studied the current distributions during electrical stimulation of the cochlear banded electrode array. They conducted the study with a tank model. The model consisted of a 22-band electrode array, each band being 0.66 mm in diameter 0.3 mm in width and separated from its adjacent band by 0.45 mm lying in the base of a tube 5 mm in diameter and 4 cm in length. The tube was filled with a homogenous normal saline solution. A probe electrode, 25 micrometer in diameter, was used to measure potential differences between the point at which the probe lies and a remotely situated gross reference

current levels are required for narrow inter-electrode spacings than for broader inter-electrode spacings. Current distributions measured by simultaneously stimulating two pairs of electrodes demonstrate a point by point vector summation of the current densities that would be obtained by independent stimulation of each of the individual pairs of electrodes. As radial distance from the array is increased, in-phase stimulation would produce a current distribution that would demonstrate a notch in the region between the 2 pairs of electrodes, whereas out-of-phase stimulation produces a bell-shaped current distribution. These results indicate the importance of knowing the distance between the array and the stimulated nerves when considering both complicated and simple forms of stimulus parameters.

Kauffmann and Achilles (1987) investigated the spread of potentials around electrode tips using a computer model based on material data extracted from the literature since they were interested in the attenuation of stimuli in the near field, as well as the different attenuation of the spectral components of the stimuli. First results using data on the acoustic nerve showed low pass filtering effects i.e., transients of the signal diminished more progressively with increasing distance than did low

frequency components. A careful control of the mutual interdependence between source resistance and stimulus waveform with given distance to the site to be stimulated was recommended. If the transients of stimulation exceed a certain level, the biomaterial around the stimulating electrode will turn progressively toward lower permittivity, in turn allowing these transients to proceed further and reach progressively more excitable fibers.

Black & Clark (1980) used a 3-dimensional electrical resistance model of the cochlea to estimate the spatial distribution of potentials and currents within the electrically stimulated cochlea. The resistance model as shown in Fig. 4.1 consists of R1 to R6 transverse elements and R7 to R10 longitudinal elements which resistively couple 16 transverse model sections together, and represent the longitudinal resistance in the cochlea. The electrical properties of different parts of the cochlea were thus analysed in separate computations by assigning the model with element values appropriate to the particular part considered. Kirchoff's laws enabled the equations to be written for computing the mesh currents around each loop in the model. The model predicts that the current distributions in the nerve fibers within the organ of Corti and also in the nerve fibres within the cochlear grounding paths are frequently different from the potential distributions measured in the scalar fluids.

Physiological experiments were also performed to measure the spread of current in the region of the terminal auditory nerve fibres which indicate that bipolar stimulation of the scala tympani results in the greatest localization of current at the stimulus site and should be considered in future designs of the multichannel cochlear prosthesis.

White and von Compernelle (1987) studied the problem of current spreading especially for scala tympani electrodes which cause a blurring of spectral features delivered to the electrode array at the somewhat remote neural tissue (the dendrites & ganglia of the auditory nerve). In their view, if current spreading is accurately known, it is possible to generate stimulation patterns at a multielectrode array that will represent faithfully considerable spectral differentiation at neural tissue. If current spreading falls within reasonable limits and current deconvolution is feasible, multichannel bandpass analog speech processors may deliver spatially differentiated neural stimulation patterns not possible otherwise. If such current deconvolution is used, it is implemented as a matrix multiplication that converts the spectral energy pattern to an electrode current specification.

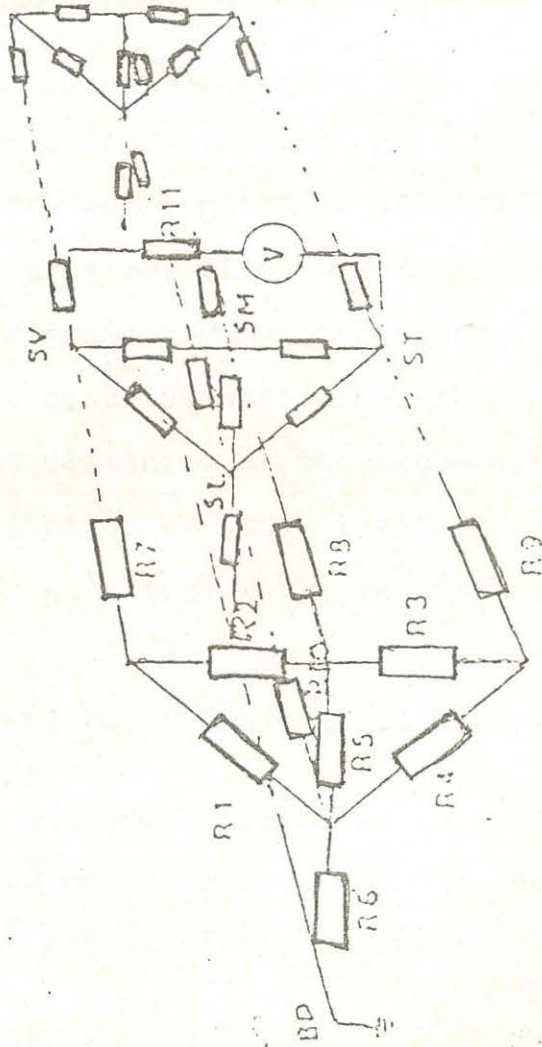


Fig. 4.1 Discrete Resistance model  
Source : Black (1980)

## CHAPTER 5

## STUDY OF POTENTIAL DISTRIBUTION

## 5.1 INTRODUCTION

This chapter describes the experiments undertaken in our study for studying the current spread behaviour under different conditions of fluid conductivity, model geometry & stimulation (waveform, rms, voltage, frequency). The experiments involve measuring the potential difference between a probe electrode and the return electrode for different distances of the probe electrode from the active electrode. Study involved varying only one parameter at a time while keeping others constant.

## 5.2 MODELS FOR POTENTIAL DISTRIBUTION STUDY

The study was conducted in two parts. In the first part, tank models were used. In the second part we used scaled-up models of the cochlea.

## 5.2.1 TANK MODELS

The models of the following shapes and dimensions are used in our study,

1. Stainless steel cylindrical tank model of diameter 18 cm and height 7.5 cm. It has a screw attached to it by way of a hole drilled on its upper part. The ground terminal of a signal generator is connected to it by insulated wire during monopolar stimulation as shown in Fig. 5.1. This model was selected as the simplest geometry for stimulation and also for studying the current spread in the far-off regions from the active electrode.

2. A 'hemicone' (a cone cut along longitudinal axis) of length 17 cm and radii at the two ends equal to 9.5 cm and 3.5 cm, with an angulation of 88.5 degrees from the vertical plane as shown in Fig. 5.2. This was made out of non-conducting polyethylene. The angulation corresponds to that of the scala tympani in the first turn of the cochlea.

3. A 'hemicylinder' (a cylinder cut along its longitudinal axis) of length 48 cm and diameter 4.4 cm as shown in Fig. 5.3. This was made out of acrylic (methyl methacrylate). The geometry corresponds to that of the scala tympani in second and third turns of the cochlea.

The above models were then placed inside freshly prepared plaster of paris to make a similar shaped mould and to give support to the model. The two open ends were closed on the sides using acrylic pieces of appropriate sizes. The models can now be placed on a horizontal plane with a fluid inside them without the danger of the fluid leaking out of the models.

When using these models in monopolar stimulation configuration, a thin aluminium foil is pressed into these vessels and cut along the borders of the vessel so that it attains the shape of the respective vessel. One end of the aluminium foil is then connected to the reference electrode with the help of a metal clip. With this arrangement, the model wall serves as a conductor and the return electrode.

#### 5.2.2 SCALED-UP SCALA TYMPANI MODELS

Since it is difficult to carry out experiments in the real-size model of the cochlea, a larger model can be built and the values for the normal size can be calculated from the data obtained with the larger model.

The approach of dimensional analysis can be used for the scaling of the model (Bekeşy 1960). If  $V_1$  is the voltage of the waveform,  $V_2$  is the voltage between the measuring electrodes,  $\sigma$  the conductivity of the fluid in the tube,  $r$  the radius of the tube, and  $l$  the length of the fluid column then the attenuation  $V_1/V_2$  is a function of the above 3 factors. Since the ratio of the two voltages is dimensionless, only the ratio  $l/r$  can appear in the expression for the function i.e.  $V_1/V_2 = f(l/r)$ . It is therefore possible to use measurements on a large tube to evaluate the effect in a small tube, as long as the length

to radius ratio is maintained constant.

Two physical models of the scala tympani were constructed. For this, first the dimensions of the cochlea was obtained from literature (Zemlin, 1985). The dimensions of the cochlea when stretched out lengthwise are shown in Fig. 5.4. It is seen that the cochlea looks like being made by joining two tubes of different geometries. The sharp angles made by the first turn of the scala tympani were calculated from the radii at two adjacent angulations. Now the length of a particular segment and its radii at either ends were calculated. For the model, the length and radii were scaled up twenty times, thus maintaining the original angulations of the scala tympani. In the process, the resistance of each of the five segments decreased by a factor of nearly twenty. With these dimensions, it was possible to construct a model of the first turn of the scala tympani. This was made by joining cut parts of conical vessels of appropriate dimensions. These vessels are made of high density polyethylene. The model was placed in a plaster of paris rectangular mould and the two open ends were closed using acrylic pieces of appropriate sizes. For the second turn of the scala tympani, we had to scale up the second model thirty times the actual dimensions, because it was difficult in our set up to use the model whose radius was only 1.1 cm.

This was made of acrylic (methyl metha-acrylate). The materials were selected mainly because of availability for the appropriate sizes and machinability. The model walls in all these cases are insulating as opposed to steel tank model where the model wall can be treated as conducting surface.

### 5.3 EXPERIMENTAL SET-UP

In our study we adopted the method of plotting the electric potential differences for measuring the current spread.

A 40 cm x 30 cm rectangular rigid plate of acrylic of 13 mm thickness was pasted with a graph paper on one surface. Holes of 1.5 mm diameter were drilled through its thickness at 5 mm intervals along two perpendicular axes. This plate was placed on the stainless vessel during the experiments and serves to hold the electrodes at known distances. For other models similar rectangular plates of appropriate sizes with holes drilled in the same fashion were used.

Thin capillary glass tube of bore 1 mm and length 10 cm was used, and a stainless steel wire of diameter 0.25 mm was passed along its length, with only the tip of the wire protruding out of the lower end of the tube. The other end of the wire was wound around the glass tube so as to fix the steel wire within the capillary tube. Plaster strip of small width was wound around the outer surface of the glass capillary tube so that only known length of the capillary tube remained below the plaster. The plaster strip served to hold the tube in place inside the holes as shown in Fig. 5.1. Two such capillary tubes were now passed through the holes in the acrylic plate so that the lower tip of the wire and glass tube acted as a electrode and were in the same plane, i.e., at the same depth.

The vessel was filled to the brim with conducting fluid of selected conductivity. The conducting fluid used in the our experiments is NaCl solution. The conductivity of the solution was verified by using a conductivity bridge.

The experimental set-up with the steel tank model is shown in Fig. 5.1. The steel wire through one of the capillary tubes was connected to the output terminal of a signal generator with the help of a metal clip. The

two terminals of a digital voltmeter V1 were connected to the active electrode and the ground of the signal generator with the help of metal clips. This voltmeter monitored the output of the signal generator. The second capillary tube with its steel wire was used as a probe electrode, the other end of which was connected to a digital voltmeter V2 which displayed the potential differences between the probe and the reference. The ground of V2 was connected to the common ground of the signal generator and V1. A photograph of the set-up is shown in Fig. 5.8.

The active electrode was placed inside one of the holes in the acrylic plate and was not moved till one full set of readings was completed. The probe electrode was placed at successive intervals of 0.5 cm from the active electrode and the potential difference across it and the reference at each of these points was noted down. These potential differences were plotted against the probe distances from the active electrode. Experiment was repeated with voltage, frequency, waveform, conductivity of the fluid, geometry of the vessel, and the stimulation configuration as a parameter (one at a time).

During bipolar stimulation, the active and the reference electrodes were kept adjacent to each other and the vessel wall is no longer in the circuit, as shown in Fig 5.7. The aluminium foil which covered the walls was removed. Similar runs were initiated and the potential difference across the probe electrode and the reference was noted down in each case. Each of the above parameters were varied and graphs plotted.

#### 5.4 EFFECT OF FLUID CONDUCTIVITY

In this experiment, we used a simplified physical model, i.e., the steel cylindrical vessel of 18 cm diameter and 8 cm height. The experiment was first conducted as described in the previous section using monopolar stimulation. The active and probe electrode tips were placed at the same depth from the surface. The stimulation was a sinusoidal waveform of 500 Hz and 3 V rms.

Experiments were conducted using NaCl solutions of five different conductivities:  $0.046\sigma_{\text{csf}}$ ,  $0.31\sigma_{\text{csf}}$ ,  $0.61\sigma_{\text{csf}}$ ,  $1\sigma_{\text{csf}}$  and  $1.48\sigma_{\text{csf}}$  mS/cm. The lowest conductivity fluid is the distilled water available in the laboratory. 15.4 mS/cm corresponds to that of the cerebrospinal fluid. Conductivity values used

here are given as a fraction of cerebrospinal fluid conductivity ( $\sigma_{csf}$ ) in Table 5.1.

### 5.5 EFFECT OF MODEL GEOMETRY

This experiment was conducted using fluid with conductivity of 15.4 mS/cm ( $\sigma_{csf}$ ) and sinusoidal waveform of 500 Hz and 3 V rms.

Physical models of different geometries were used during each of the following runs. Thus three runs were initiated using a steel cylindrical model, hemi-conical model and the hemicylindrical model.

The potential differences at different distances from the active electrode were noted down during monopolar stimulation. While using the polyethylene and acrylic models, a thin sheet of aluminium foil was pressed into the vessel and the foil was cut at the vessel boundaries so that the foil assumes the form of the vessel. This foil serving as the conducting wall for the model, was connected to the reference with the help of a metal clip. It was made sure that the two electrodes were placed at the same depth from the surface. Similar runs were made with bipolar stimulation configuration, except that the aluminium foil was not placed, i.e., wall surface was non-conducting.

## 5.6 EFFECT OF STIMULATION WAVEFORM

The effect of different types of stimulation waveform on the potential distribution is studied in this experiment using the fluid conductivity of 15.4 mS/cm (corresponding to that of the CSF) and the steel cylinder vessel.

In the first part of the experiment, the stimulation was 500 Hz and 3 v rms. Two runs were made, one using sinusoidal waveform and the other using square waveform. The rms values of potential differences were noted down for the different distances from the active electrode in monopolar configuration.

In the second part, 3 V rms sinusoidal waveform was used at five different frequencies : 0.01, 0.10, 0.50, 1.0, and 10 kHz. The potential difference between the probe and reference was noted at different distances from the active electrode and plotted. The same was repeated using bipolar configuration.

In the third part of this experiment, the rms value of the sinusoidal waveform of 500 Hz was varied. Four runs were made using 1, 3, 5 and 7 V. The procedure was repeated using bipolar electrode configuration.

## 5.7 EFFECT OF ELECTRODE CONFIGURATION

In this experiment, the conductivity of the fluid, the excitation waveform, frequency and voltage were kept constant and all measurements were made in the steel cylinder model. Two experiments were carried out using monopolar and bipolar electrode configurations.

## 5.8 STUDY WITH SCALED UP PHYSICAL MODELS

If the cochlea is unwound and stretched out longitudinally we find that it is about 31 mm long and appears to be made up of two types of tubes (Zemlin, 1985). The first turn of the cochlea which is 15.5 mm in length appears irregular in outline with six sharp angulations and the second tube consisting of the second and third turn is together 15.5 mm in length and is cylindrical. With the help of the areas given at the different angles we can calculate the radii at these points and thereby the degree of angulation. Having found out these dimensions, two scaled up physical models of the scala tympani compartment were constructed using non-conducting materials, high density polyethylene and acrylic (methyl methacrylate) as discussed earlier in section 5.2.2. A photograph of the scala tympani model (first turn) is shown in Fig 5.9.

In this experiment, we placed a the active electrode at the different angles in the first model and measured potential differences from the active electrode at different distances. This was first done in monopolar stimulation configuration. A thin sheet of aluminium foil was pressed into the model so that it lay on the walls of the model and assumed the shape of the model. The aluminium foil, serving as the conducting wall surface, was connected to the reference electrode with the help of a metal clip. The excitation waveform was a sinusoid of 500 Hz and 3 volts (rms). The measurements were made with the fluid conductivity of 15.4 mS/cm. Six runs were made, each time keeping the active electrode at one of the angulation. The electrode tips were at the depth of 2.5 cm from the surface of the fluid. Plots were drawn for potential difference against distance from the active electrode. The same procedure was repeated using bipolar electrode configuration. Similar readings were taken for the model of the second tube.

TABLE 5.1

Fluid conductivities ( $\sigma$ ) used in the experiments, expressed as a fraction of the conductivity of cerebrospinal fluid ( $\sigma_c = 15.4$  mS/cm).

	( $\sigma$ in mS/cm)	$\sigma/\sigma_c$
1.	0.56	0.046
2.	4.65	0.310
3.	9.38	0.610
4.	15.40	1.000
5.	22.85	1.480

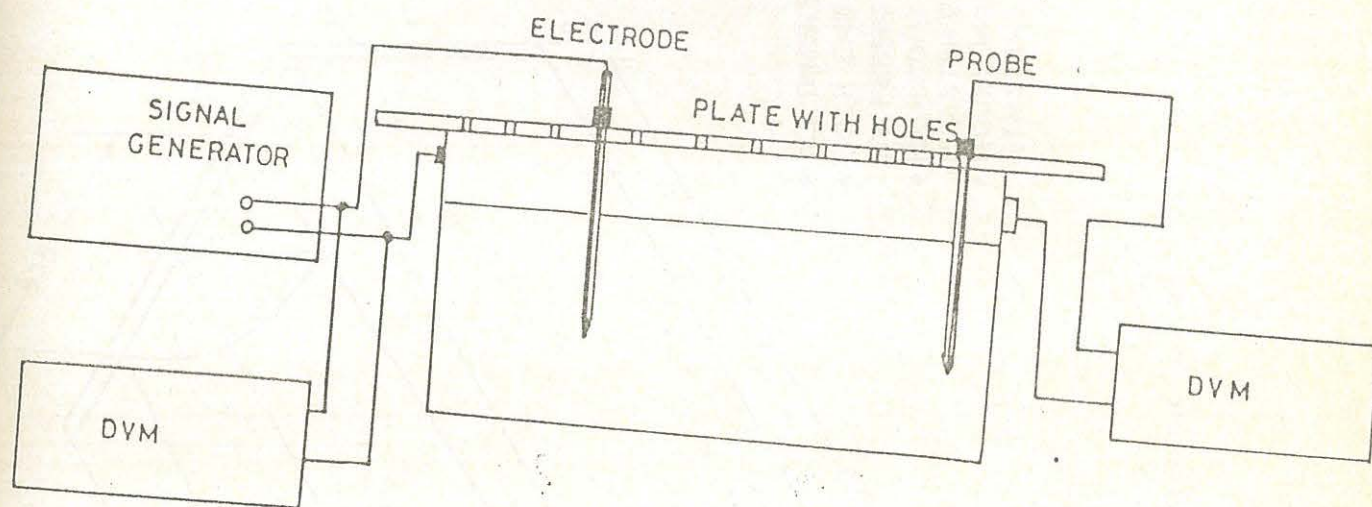
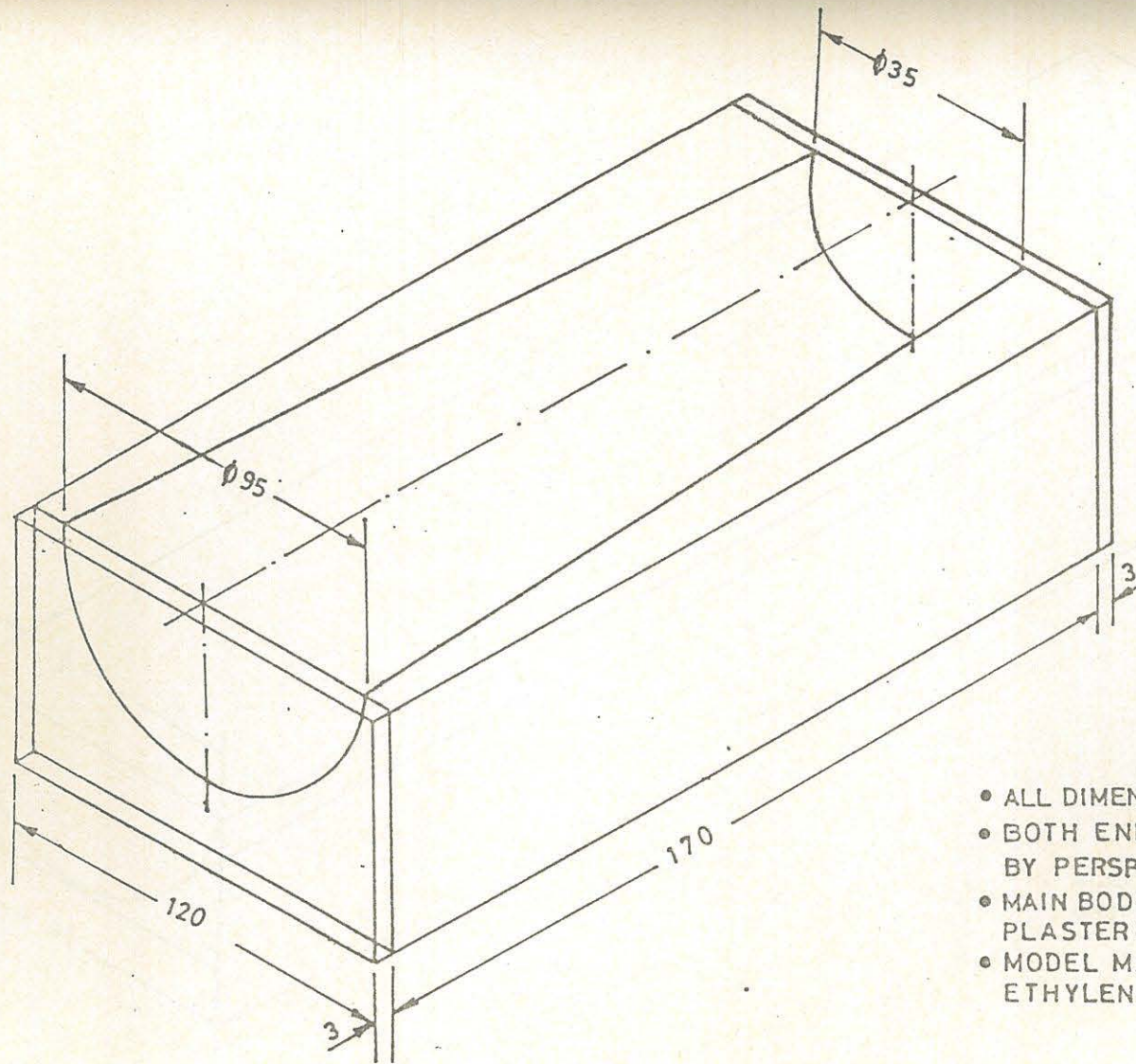
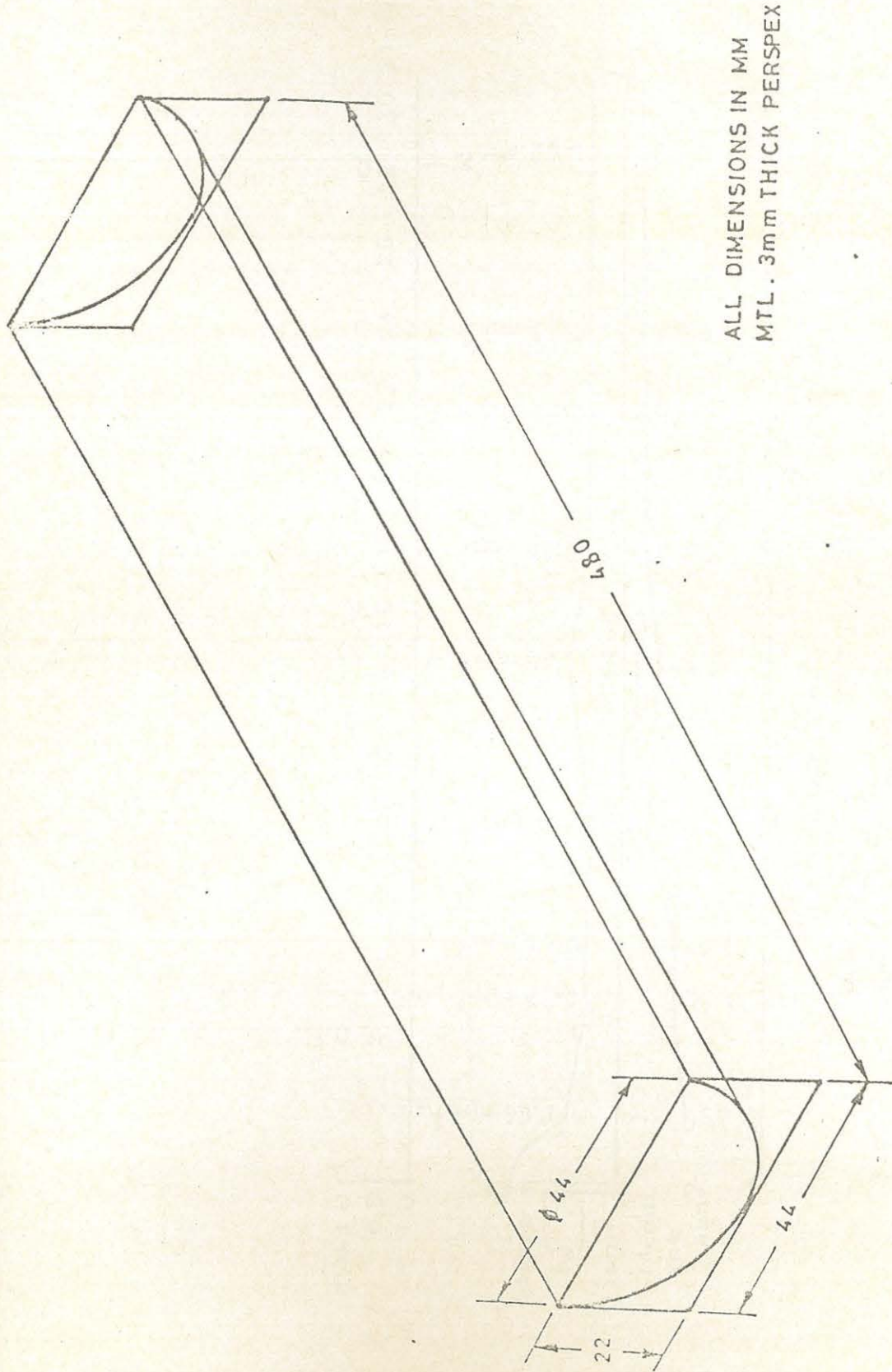


FIG. 5. 1. THE EXPERIMENTAL SET UP



- ALL DIMENSIONS IN MM
- BOTH ENDS ARE CLOSED BY PERSPEX SHEET.
- MAIN BODY IS MADE BY PLASTER OF PARIS
- MODEL MADE OF H.D. POLY ETHYLENE

Fig.5.2. A hemicone model.



ALL DIMENSIONS IN MM  
MTL. 3mm THICK PERSPEX

FIG. 5.3. A hemicylindrical model.

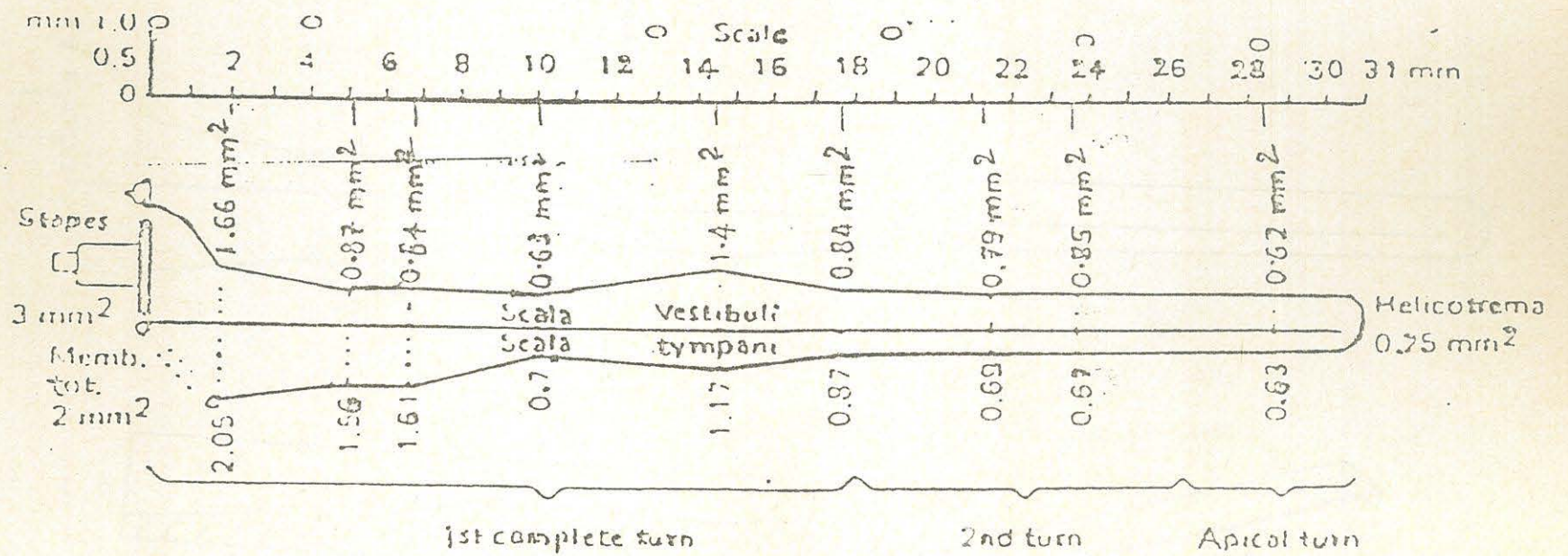


Fig.5.4. Dimensions of the cochlea. Source: Zemlin (1985).

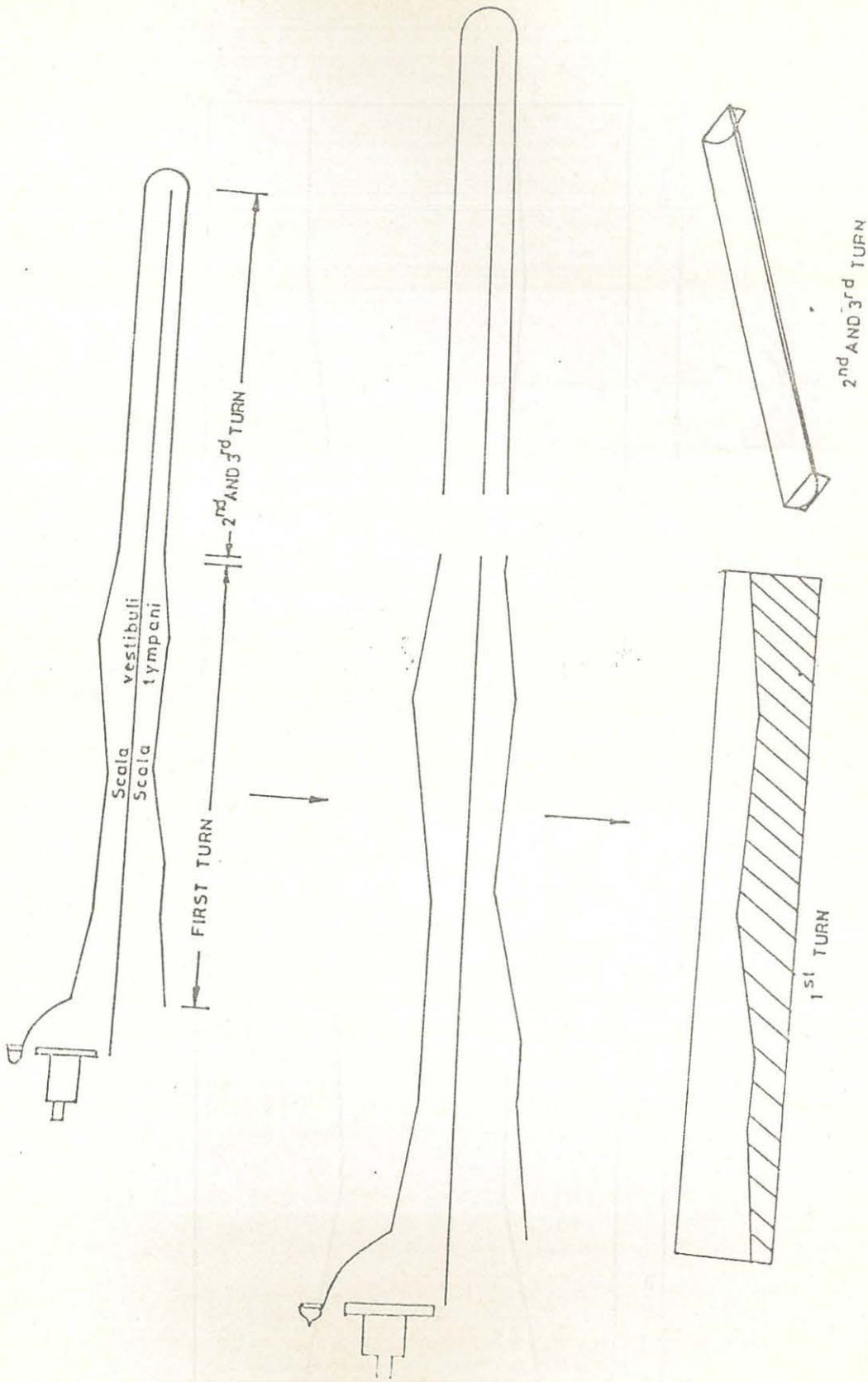


FIG. 5. 5. Modelling of the scala tympani.

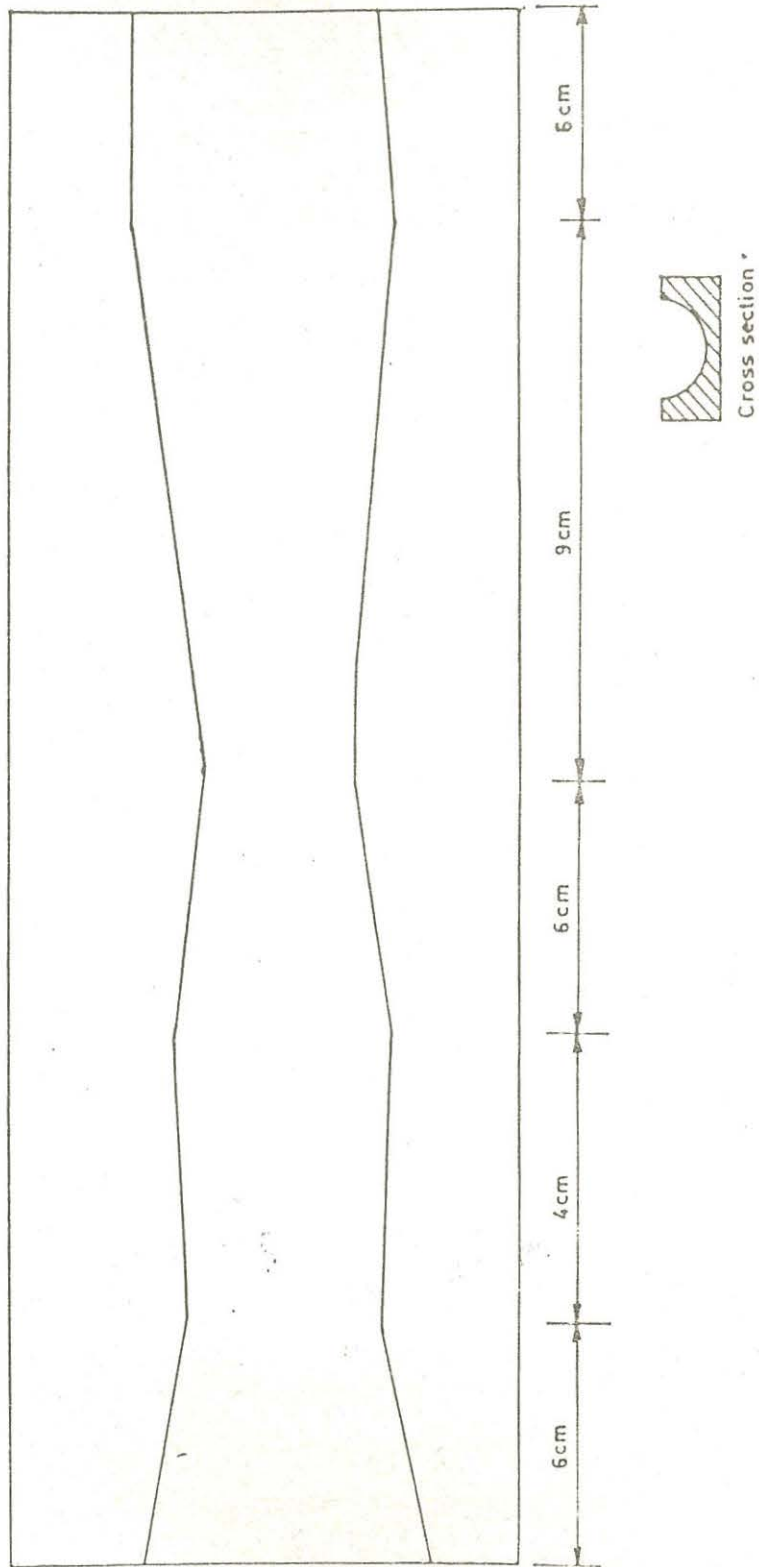
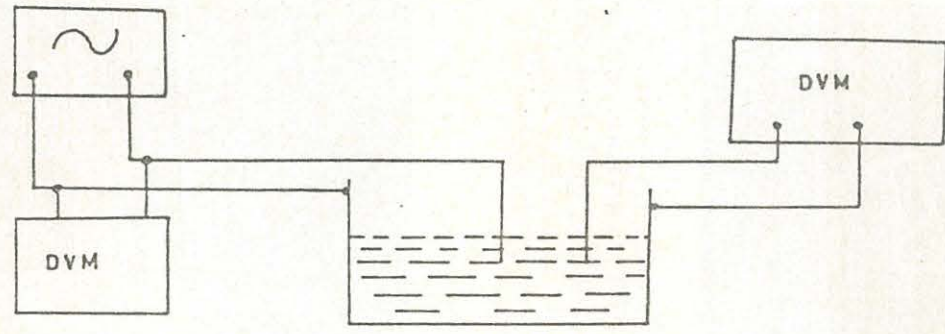
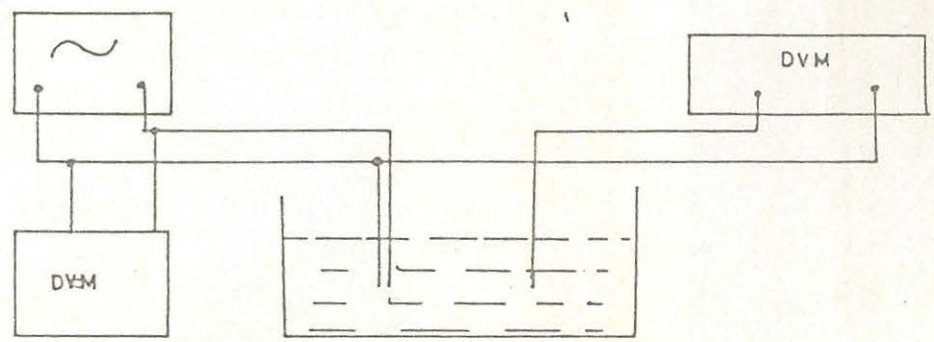


FIG. 5.6. A scala tympani model.



MONOPOLAR STIMULATION



BIPOLAR STIMULATION

Fig. 5.7 The two different electrode configurations

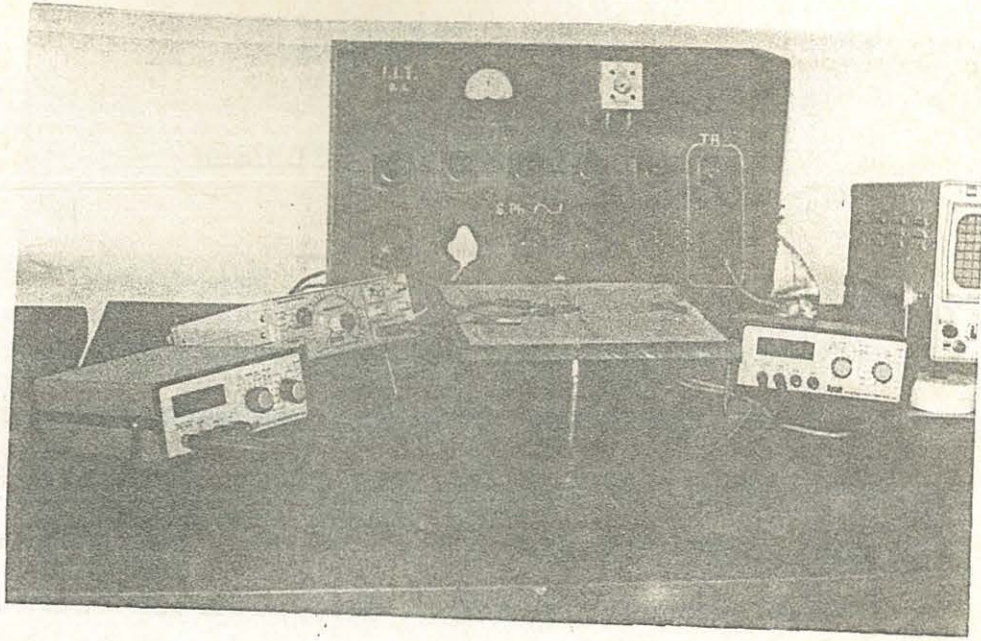


Fig. 5.8. Photo of the Experimental set-up. Seen are the acrylic plate with holes, electrodes, digital voltmeters, signal generator and the circular vessel.

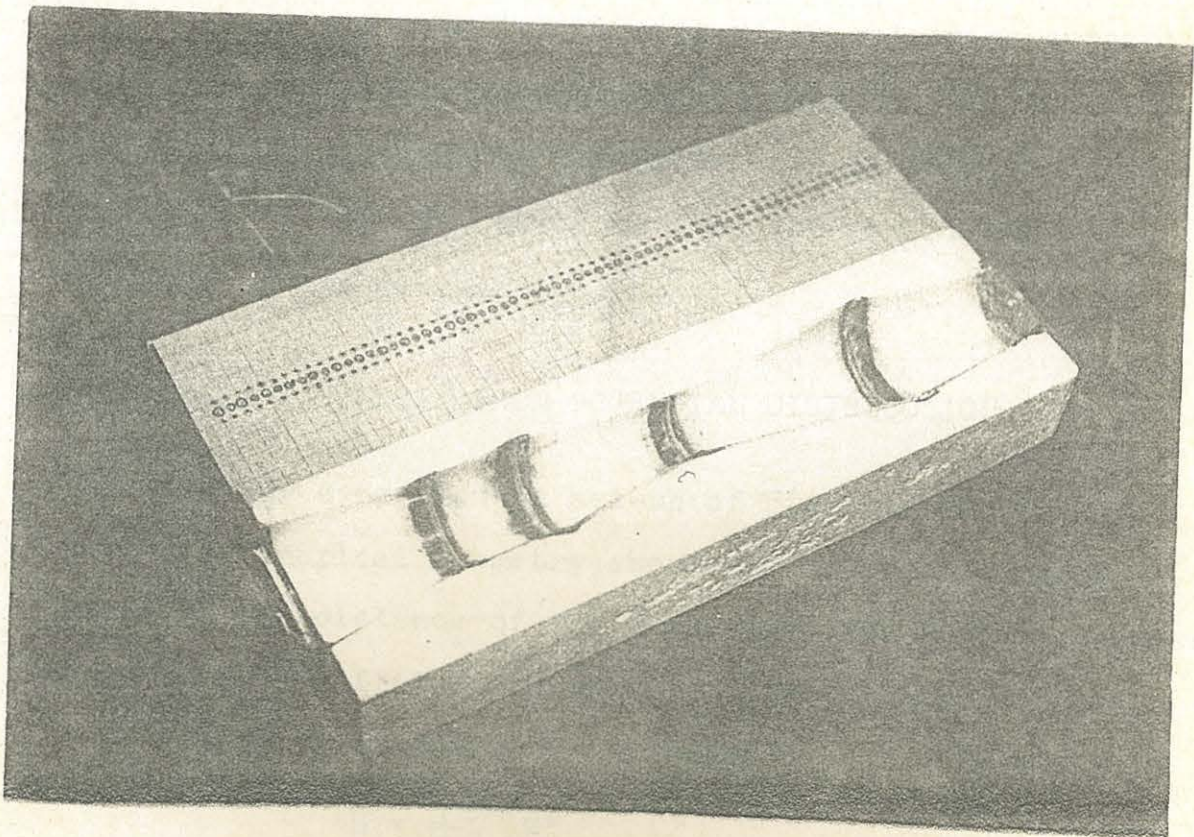


Fig. 5.9 Photo of the scala tympani model (first turn). Seen also are the rectangular plate with holes and electrodes.

## CHAPTER 6

## RESULTS AND ANALYSIS

## 6.1 INTRODUCTION

In our experiments, we have used alternating current stimulation (in 10 Hz to 10 kHz frequency range) and relatively small excitation levels (rms value not exceeding 7v). We were concerned with measuring the potential distributions around electrodes under different condition of fluid conductivity, model geometry, stimulation (waveform, rms voltage, frequency) and electrode configuration.

In the next section, a method for obtaining current density from potential distribution will be outlined. This will be followed by the presentation, analysis, and discussion of results obtained from the experiments outlined in the preceding chapter.

## 6.2 CURRENT DENSITY FROM POTENTIAL DISTRIBUTION

In our experimental set-up of Fig 5.1, we can assume cylindrical symmetry about the active electrode. Let  $r$  be the distance of the probe from the active electrode, and  $\sigma$  be the fluid conductivity. Then the resistance  $R$  of a thin fluid sheet of thickness  $dr$  and length  $l$  will be

$$R = \frac{l}{\sigma} \cdot \frac{dr}{2\pi r l}$$

If  $I$  be the current crossing the sheet, then the potential difference  $\phi$  across this sheet will be

$$d\phi = I R$$

Therefore the current density over the surface of the cylindrical sheet will be

$$J = \frac{I}{2 \pi r l}$$

or  $J = \sigma \frac{d\phi}{dr} \quad \dots (6.1)$

Therefore if we have  $\phi$  available as a function of  $r$ , we can find the current density  $J$  also as a function of  $r$ .

Grapher (C) 1986 package (from Golden Software) was used to obtain a numerical best fit curve for experimentally measured potential difference values  $\phi(r)$ .

The following alternatives are available in this package:

- |                |                               |
|----------------|-------------------------------|
| 1. linear      | $\phi = a + br$               |
| 2. Logarithmic | $\phi = a + b \log r$         |
| 3. exponential | $\phi = a + b \exp (cr)$      |
| 4. Power       | $\phi = a + b (r)^c$          |
| 5. Cubic       | $\phi = a + br + Cr^2 + dr^3$ |

The package shows the actual plot and the best fit curve for each alternative. For each curve, the best fitting alternative was taken. This can be used for obtaining the derivative of  $\phi$  with respect to  $r$  and thereby we can obtain the current density  $J(r)$  from the potential function  $\phi(r)$  by making use of the equation 6.1

### 6.3 EFFECT OF FLUID CONDUCTIVITY

The values of potential difference between the probe and the return electrode,  $\phi$ ,  $r$  as a function of the distance of the probe from the active electrode  $r$ , for monopolar configuration in the steel tank model for the different fluid conductivities are given in Table 6.1 a and plotted in Fig 6.1. At higher fluid conductivities, the potentials decay faster and this shows some amount of localisation of the stimulus. As expected, the higher fluid conductivities result in larger current densities (we have employed voltage stimulus). The decay rates for the current densities for different conductivities are not much different, except for the case of the lowest conductivity. Numerically best fitting curves, and the expression for the current density calculated therefrom are given in Table 6.1.b.

For bipolar stimulation, the separation between the active and the return electrode is less than 1 mm. The value of the potential difference as a function of the distance, measured around the two electrodes, are given in the Table 6.2 and plotted in Fig. 6.2. We observe equipotential distribution. Therefore, in the range of conductivities used in the experiment and in the region outside the immediate vicinity of the electrode pair, the current density can be assumed to be zero.

#### 6.4 EFFECT OF MODEL GEOMETRY

The values of potential difference between the probe and the return electrode ( $\phi$ ) as a function of distance of the probe from the active electrode, for monopolar electrode configuration in the different models for fluid conductivity of 15.4 mS/cm are given in the Table 6.3 and plotted in Fig 6.3. In the case of the hemicylinder model shown in Fig 5.3, the potential differences fall very steeply initially but the fall is less steep for distances more than 4 cm from the active electrode. This indicates more localisation of current near the active electrode and less spreading of current. The curves for the other model geometries occupy positions which indicate relatively more spreading of current in the surrounding region. Numerically best fitting curves are given in table 6.2

## 6.5 EFFECT OF STIMULATION WAVEFORM

The values of potential differences between the probe and the return electrode ( $\phi$ ) as a function of distance of the probe from the active electrode  $r$ , for monopolar electrode configuration in the cylindrical steel tank model for fluid conductivity of 15.4 mS/cm under different conditions of stimulation (waveform, rms voltage, frequency) are given in Tables 6.4, 6.5, and plotted in Figs 6.4, 6.5 and 6.6. Numerically best fitting curves and the expression for current density calculated therefrom are given in Tables 6.4 a, 6.5.a, and 6.6.a.

In the case of square waveforms the potential differences are higher than for the sinusoidal waveforms. In the plots for the rms value of waveforms, we see that for 1 v rms, there is less change in the potential differences after a short distance from the active electrode showing that there is less spreading. For higher voltage waveforms the current spreading is more. From the plots for waveforms of different frequencies as shown in Fig. 6.5 we see that the curve for 1 and 10 kHz show a steep fall in the potential upto 1 cm from the active electrode, then a relatively less steep slope upto 5 cm from the electrode and thereafter very little change. It appears that around the electrode the stimulus

gets more localised and less spreading occurs as we increase the frequency from 100 to 500 Hz.

#### 6.6 EFFECT OF ELECTRODE CONFIGURATION

Referring to Table 6.1 and 6.2 we can see that for monopolar electrode configuration the potential differences recorded are in millivolts and keeps falling as we move further away from the active electrode. For bipolar electrode configuration, the values of the potential differences are more than a volt but remains equipotential. It can be assumed that the current density in the immediate vicinity of the electrode pair, is zero.

#### 6.6 CURRENT SPREAD IN THE SCALA TYMPANI MODELS

The curves obtained with the potential differences ( $\phi$ ) as a function of distance  $r$  from the active electrode during monopolar stimulation for fluid conductivity of 15.4 mS/cm are given in Table 6.8 and plotted in Fig 6.8. The electrode is placed at the different distances A,B,C,D,E, and F from the basal end in the physical model of the first turn of the scala tympani. Numerically best fitting curves are given in Table 6.8.b. All the curves follow exponential patterns. The curve for the second model of the scala tympani shows steep fall upto 1 cm from the active electrode and a less steep fall upto 4 cm from the active electrode after which the fall is very little.

TABLE - 6.1. a

Effect of fluid conductivity in steel tank model under  
monopolar electrode configuration  
Stimulus : 500 Hz, 3V rms sinusoidal

$r$  = probe distance from the active electrode, in cm

$\phi$  = potential difference between the probe and the  
return electrode, in mV

$\sigma$  = fluid conductivity, in mS/cm

$r$	$\phi$				
	$\sigma = 0.56$	$\sigma = 4.65$	$\sigma = 9.38$	$\sigma = 15.4$	$\sigma = 22.85$
0.5	186.0	78.0	51.0	53.6	61.0
1.0	103.0	44.0	31.0	29.6	43.0
1.5	66.5	30.0	21.2	25.5	30.5
2.0	49.0	22.0	17.0	19.6	23.7
2.5	37.5	16.0	13.5	15.5	19.4
3.0	28.6	12.0	10.3	12.6	14.5
3.5	22.8	9.0	7.6	9.5	12.5
4.0	19.4	7.3	7.0	7.8	10.0
4.5	15.2	5.7	6.0	6.0	9.0
5.0	12.2	4.8	5.1	5.0	7.5
5.5	10.2	4.0	4.5	5.4	6.5
6.0	8.0	3.2	4.1	3.4	5.5
6.5	6.6	2.6	3.4	3.1	4.8
7.0	5.1	2.2	2.8	2.8	4.1
7.5	4.5	1.8	2.3	2.4	3.6
8.0	3.6	1.6	2.0	2.1	3.2

TABLE 6.1.b

Numerically best fit curve for potential  $\phi(r)$  and current density  $J(r)$  for the steel tank model (monopolar electrode configuration, 500 Hz, 3V rms sinusoid stimulus).

$\sigma$  in mS/cm,  $\phi$  in mV,  $r$  in cm,  $J$  in mA/cm<sup>2</sup>.

Conductivity	Best fit curve for $\phi(r)$	Current density $J = d\phi/dr$
0.56	109.45 $r^{-1.44}$	-0.088 $r^{-2.44}$
4.65	46.60 $r^{-1.47}$	-0.319 $r^{-2.47}$
9.38	31.84 $r^{-1.18}$	-0.352 $r^{-2.18}$
15.40	35.30 $r^{-1.22}$	-0.663 $r^{-2.22}$
22.85	42.70 $r^{-1.12}$	-1.092 $r^{-2.12}$

TABLE 6.2

Effect of fluid conductivity on potential distribution  
in steel tank model under bipolar configuration.  
Stimulus : 500 Hz, 3V rms sinusoidal

$r$  = probe distance from the active electrode, in cm

$\phi$  = potential difference between the probe and the  
return electrode, in mV

$\sigma$  = fluid conductivity, in mS/cm

(The potential difference was found to be the same  
at different distances in the range of 0.5 to 8.0 cm)

$r$	$\phi$				
	$\sigma = 0.56$	$\sigma = 4.6$	$\sigma = 9.38$	$\sigma = 15.4$	$\sigma = 22.98$
0.5 to 8.0	1.40	1.48	1.58	1.64	1.75

TABLE 6.3.a

Effect of model geometry on potential distribution  
under monopolar electrode configuration

Stimulus : 500 Hz, 3V rms sinusoidal

Fluid conductivity  $\sigma$  : 15.4 mS/cm

$\phi$  = potential difference between the probe and the  
reference, in

r = probe distance from the active, in cm

Model geometry: hemicylinder, hemicone 1, hemicone 2  
as shown in Figs 5.1, 5.2, and 5.3

r	$\phi$		
	Hemicylinder model	Hemicone 1 $\theta = 9.5$	Hemicone 2 $\theta = 3.5$
0.5	97.5	57.5	99.0
1.0	46.8	36.5	64.5
1.5	30.5	26.2	46.2
2.0	21.0	20.9	34.5
2.5	15.3	16.5	27.0
3.0	11.5	14.0	21.5
3.5	9.0	12.5	17.5
4.0	6.8	10.4	14.0
4.5	5.6	9.0	11.5
5.0	5.1	7.7	9.5
5.5	4.6	6.7	8.0
6.0	4.4	5.8	8.3
6.5	4.1	5.0	6.0
7.0	3.9	4.3	5.0
7.5	3.7	3.7	4.0
8.0	3.4	3.2	3.4

TABLE 6.3 b

Numerically best fit curve for potential  $\phi(r)$  for models of different geometry under monopolar electrode configuration (500 Hz, 3V rms sinusoidal stimulus)

$\phi(r)$  in mV, r in cm

Model geometry	Best fit curve for $\phi(r)$
Hemicylinder	$45.26 r^{-1.3}$
Hemicone 1	$37.87 r^{-1.1}$
Hemicone 2	$66.77 r^{-1.25}$

TABLE 6.4.a

Effect of stimulation waveform in steel tank model  
under monopolar electrode configuration

Stimulus : 500 Hz, 3V rms (Sine & Square waveform)

Fluid conductivity  $\sigma = 15.4$  mS/cm

$r$  = probe distance from the active, in cm

$\phi$  = potential difference between the probe and the  
return electrode, in mV

r	$\phi$	
	Sinusoidal waveform	Square waveform
0.5	71.0	96.0
1.0	38.0	58.0
1.5	27.0	40.0
2.0	19.5	30.0
2.5	14.7	24.0
3.0	11.8	19.0
3.5	9.6	16.0
4.0	8.4	14.2
4.5	7.2	12.5
5.0	6.7	11.0
5.5	6.0	10.0
6.0	5.4	9.0
6.5	5.0	8.0
7.0	4.7	7.6
7.5	4.7	7.0
8.0	4.5	7.0

TABLE 6.4.b

Numerically best fit curve for potential  $\phi(r)$  and current density  $J(r)$  for the steel tank model.

Monopolar electrode configuration

Stimulus : 500 Hz, 3V rms sinusoidal and square waveform

$\phi(r)$  in mV,  $r$  in cms,  $J$  in mA/cm<sup>2</sup>

Waveform	Best fit curve for $\phi(r)$	current density $J = d\phi/dr$
Sinusoidal	$37.3 r^{-1.05}$	$-0.603 r^{-2.05}$
Square	$55.9 r^{-1.00}$	$-0.862 r^{-2.00}$

TABLE 6.5

Effect of stimulation voltage in steel tank model under monopolar electrode configuration

Stimulus : 500 Hz, sinusoidal, rms of the stimulation, in V

Fluid conductivity  $\sigma = 15.4$  mS/cm

$r$  = probe distance from the active, in cm

$\phi$  = potential difference between the probe and the reference, in mV

$r$	$\phi$			
	rms = 1 V	3V	5V	7V
0.5	13.0	34.0	70.0	97.0
1.0	6.5	19.0	40.0	52.0
1.5	5.0	14.0	27.5	38.0
2.0	3.5	11.0	20.0	30.0
2.5	3.0	8.0	16.0	24.0
3.0	2.5	7.5	12.5	18.0
3.5	2.3	6.0	10.0	14.5
4.0	2.0	5.0	8.0	12.0
4.5	1.8	4.0	7.0	9.5
5.0	1.8	3.5	6.0	7.5
5.5	1.7	3.5	5.0	5.5
6.0	1.7	3.0	4.0	5.0
6.5	1.7	2.5	3.5	5.0
7.0	1.6	2.5	3.5	5.0
7.5	1.6	2.2	3.5	4.0
8.0	1.5	2.2	3.5	4.0

TABLE 6.5.b

Numerically best fit curve for potential  $\phi(r)$  and

current density  $J(r)$  for the steel tank model.

Monopolar electrode configuration for different rms value  
of the stimulus (500 Hz, sinusoidal stimulus)

$\phi(r)$  in mV,  $r$  in cms,  $J$  in mA/cm<sup>2</sup>

rms value	Best fit curve for $\phi(r)$	Current density $J = d\phi/dr$
1	$6.5 r^{-0.77}$	$-0.076 r^{-1.77}$
3	$19.8 r^{-1.04}$	$-0.317 r^{-2.04}$
5	$40.0 r^{-1.19}$	$-0.734 r^{-2.19}$
7	$57.0 r^{-1.24}$	$-1.090 r^{-2.24}$

TABLE 6.6.a

Effect of stimulation frequency in the steel tank model

under monopolar electrode configuration

Fluid conductivity  $\sigma = 15.4$  ms/cm

Stimulus: 3V rms sinusoidal,

$f$  = stimulus frequency in kHz

$r$  = probe distance from the active, in cm

$\phi$  = probe distance between the probe and the reference, in mV

$r$	$\phi$				
	$f = 0.01$	$f = 0.1$	$f = 0.5$	$f = 1.0$	$f = 10$
0.5	50.0	67.0	70.0	143.0	156.6
1.0	32.0	35.5	40.0	75.7	83.0
1.5	22.0	25.5	26.2	49.0	56.0
2.0	17.3	18.0	19.2	36.2	42.0
2.5	15.0	15.0	16.7	28.0	33.0
3.0	13.0	12.0	13.5	22.8	26.5
3.5	12.0	10.0	12.3	19.0	22.2
4.0	11.5	8.8	10.7	16.7	18.5
4.5	10.5	7.5	9.4	14.7	16.2
5.0	10.0	7.2	8.3	13.0	14.0
5.5	9.5	6.7	7.8	11.7	12.7
6.0	9.0	6.3	6.8	10.7	11.3
6.5	8.8	6.0	6.3	9.8	10.6
7.0	8.7	5.6	5.8	8.8	9.5
7.5	8.6	5.4	5.6	8.3	8.5
8.0	8.5	5.0	5.2	7.0	8.0

TABLE 6.6.b

Numerically best fit curve for potential  $\phi(r)$  and current density  $J(r)$  for the steel tank model, monopolar electrode configuration (3V rms, sinusoidal stimulus)  
 $\phi(r)$  in mV,  $r$  in cms,  $J$  in mA/cm<sup>2</sup>

Frequency in kHz	Best fit curve for $\phi(r)$	Current density $J = d\phi/dr$
0.01	29.25 $r^{-0.65}$	-0.293 $r^{-1.65}$
0.10	35.00 $r^{-0.96}$	-0.517 $r^{-1.96}$
0.50	38.39 $r^{-0.95}$	-0.561 $r^{-1.95}$
1.00	73.66 $r^{-1.00}$	-1.135 $r^{-2.08}$
10.00	83.40 $r^{-1.1}$	-1.413 $r^{-2.10}$

TABLE 6.7

Effect of electrode configuration in the steel tank model

Stimulus : 500 Hz, rms sinusoid

Fluid conductivity  $\sigma = 15.4$  mS/cm

$r$  = probe distance from the active, in cm

$\phi$  = potential difference between the probe and the reference, in mV

$r$	$\phi$	
	Monopolar	Bipolar
0.5	53.6	1.64
1.0	29.6	"
1.5	25.5	"
2.0	19.6	"
2.5	15.5	"
3.0	12.6	"
3.5	9.5	"
4.0	7.8	"
4.5	6.0	"
5.0	5.0	"
5.5	4.4	"
6.0	3.4	"
6.5	3.1	"
7.0	2.8	"
7.5	2.4	"
8.0	2.1	"

TABLE 6.8.a

Potential distributions in the study of current spread in monopolar stimulation configuration in the physical models of the scala tympani

Fluid conductivity  $\sigma = 15.4$  mS/cm

Stimulus: 500 Hz, 3V rms, sinusoidal waveform.

$\phi$  in mV, r in cms

A,B,C,D,E,F, & X are points at the angulations in the scala tympani models.

r	$\phi$						
	A	B	C	D	E	F	X
0.5	119	115	109	109	100	98	97
1.0	90	82	88	75	67	61	47
1.5	79	68	75	56	56	48	31
2.0	68	59	63	45	49	40	21
2.5	58	51	65	38	42	35	15
3.0	50	44	47	31	39	31	12
3.5	40	38	40	25	32	27	9
4.0	32	33	33	20	28	24	7
4.5	29	29	27	16	25	22	6
5.0	25	25	21	13	22	19	5
5.5	22	22	16	11	20	17	5
6.0	19	18	10	9	18	16	4
6.5	17	16	8	8	16	14	4
7.5	13	14	6	7	14	12	4
7.5	10	12	5	6	12	11	3
8.0	9	9	4	5	8	10	3

TABLE 6.8.b

Numerically best fit curve for potential  $\phi(r)$  for the scala tympani models under monopolar electrode configuration  
Stimulus: 500 Hz, 3V rms, sinusoidal waveform.

Active electrode placed at different points in the models.

A to F angulations of the scala tympani from the basal end in the first model. X is any point in the second model.

Electrode tip submerged 1 cm from the fluid surface

Location of electrode	Best fit curve for $\phi(r)$
A	132 exp (-0.333 r)
B	115 exp (-0.310 r)
C	163 exp (-0.450 r)
D	105 exp (-0.397 r)
E	92 exp (-0.283 r)
F	77 exp (-0.270 r)
X	45 r <sup>-1.3</sup>

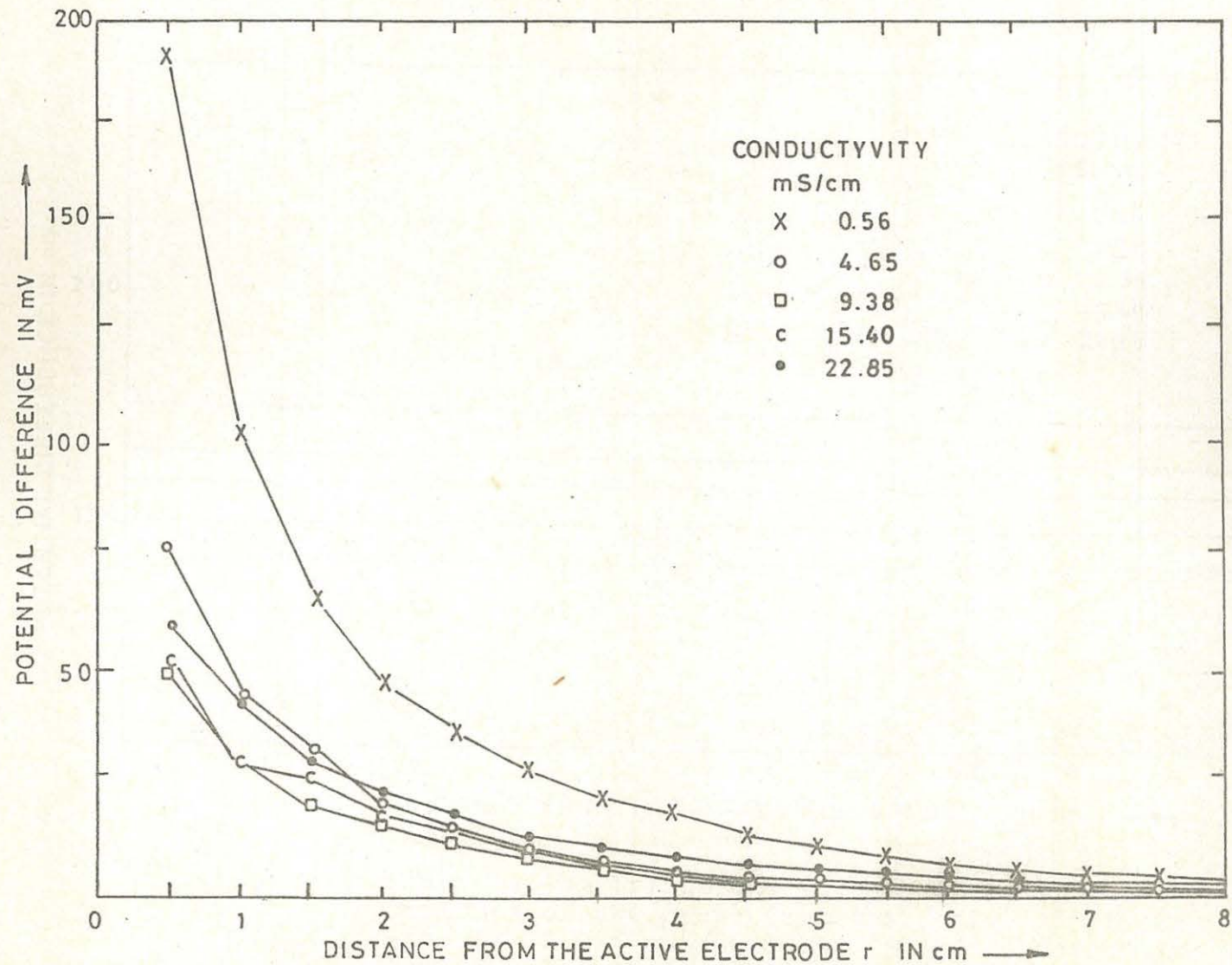


Fig. 6.1 Potential distributions ( $\phi$ ) as a function of distance of the probe from the active electrode ( $r$ ) with fluid conductivity ( $\sigma$ ) as a parameter during monopolar stimulation

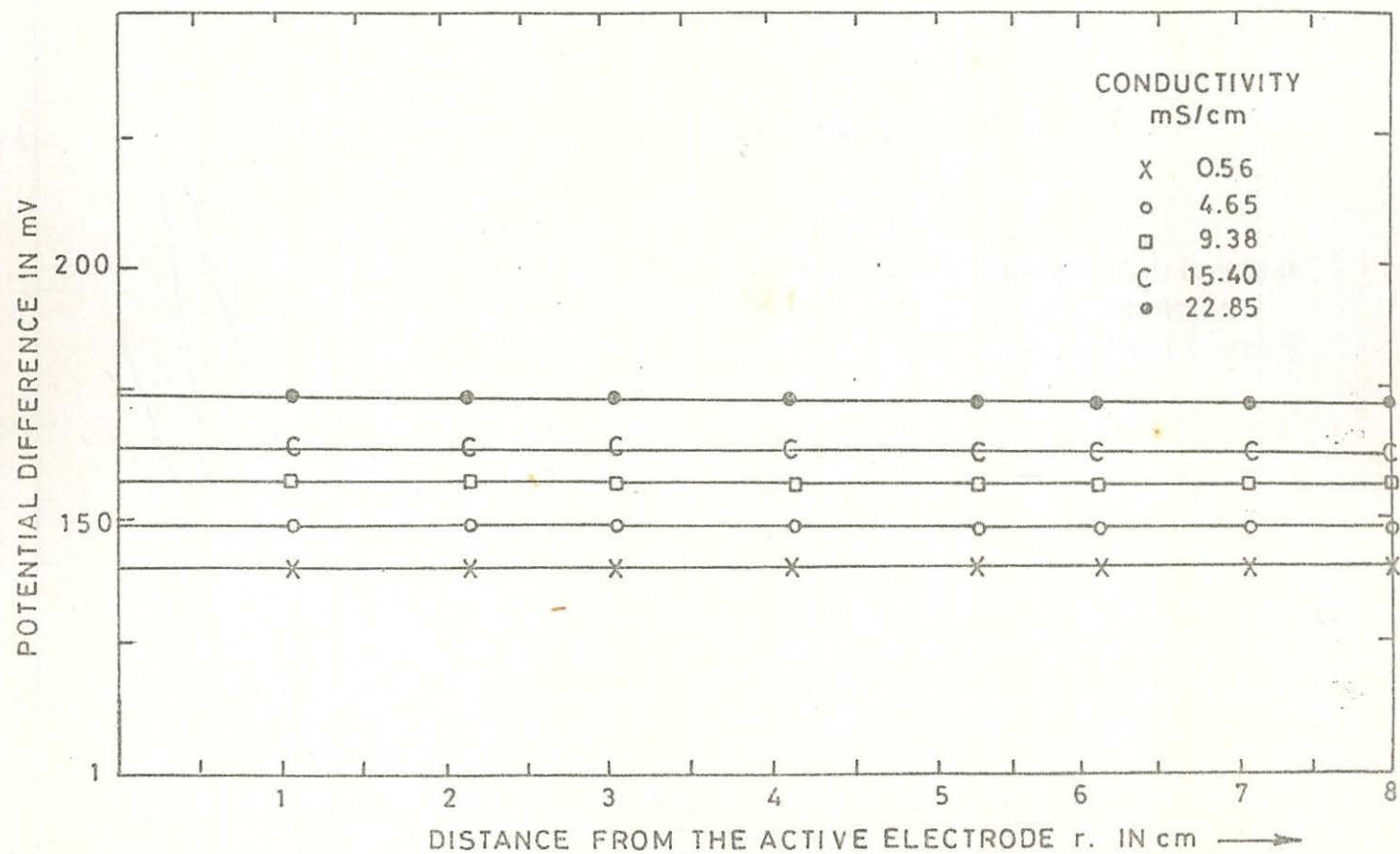


Fig. 6.2 Potential distributions ( $\phi$ ) as a function of distance of the probe from the active electrode ( $r$ ) with fluid conductivity ( $\sigma$ ) as a parameter during bipolar stimulation.

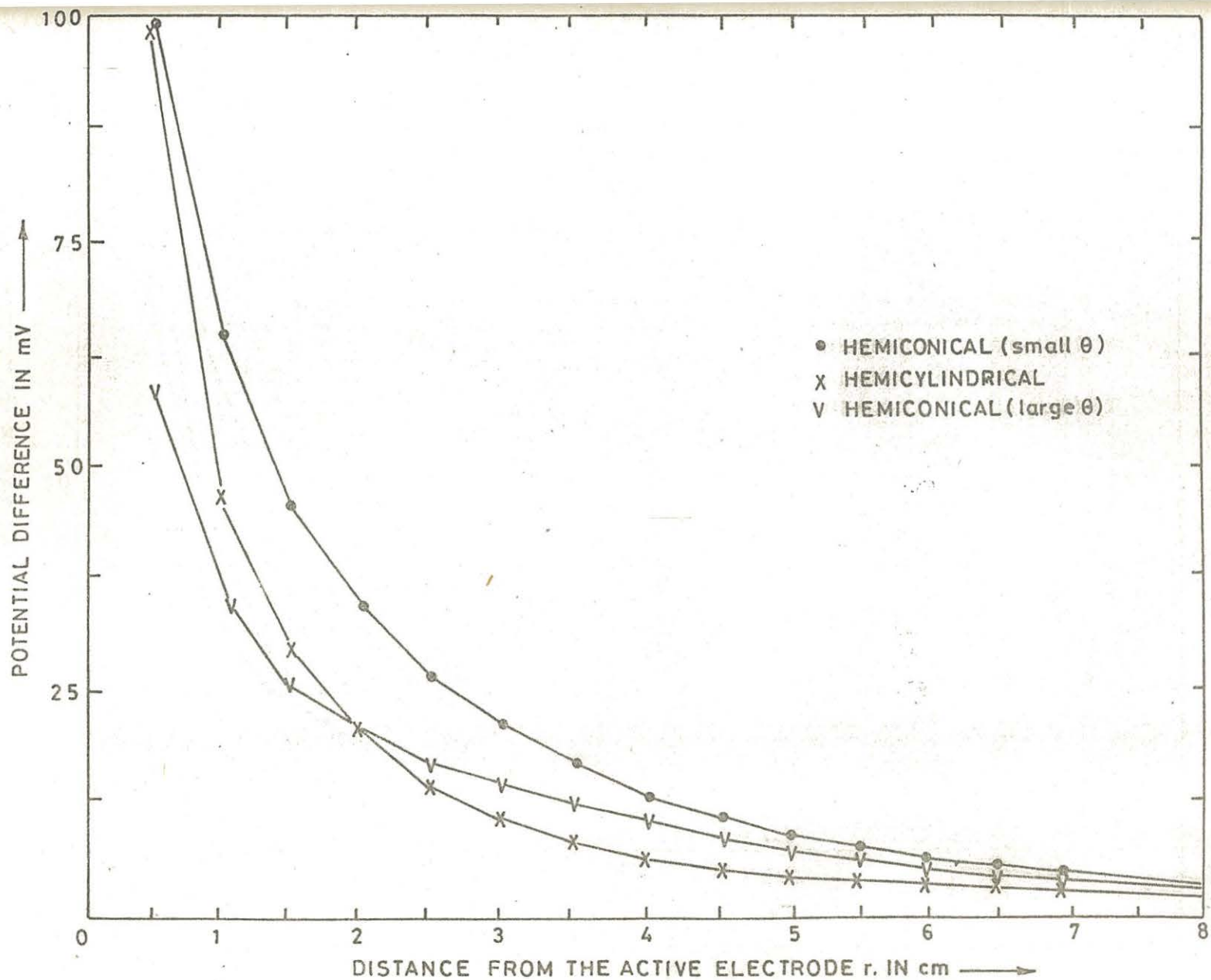


Fig. 6.3 Potential distributions ( $\phi$ ) as a function of distance of the probe from the active electrode ( $r$ ) with vessel geometry as a parameter during monopolar stimulation.

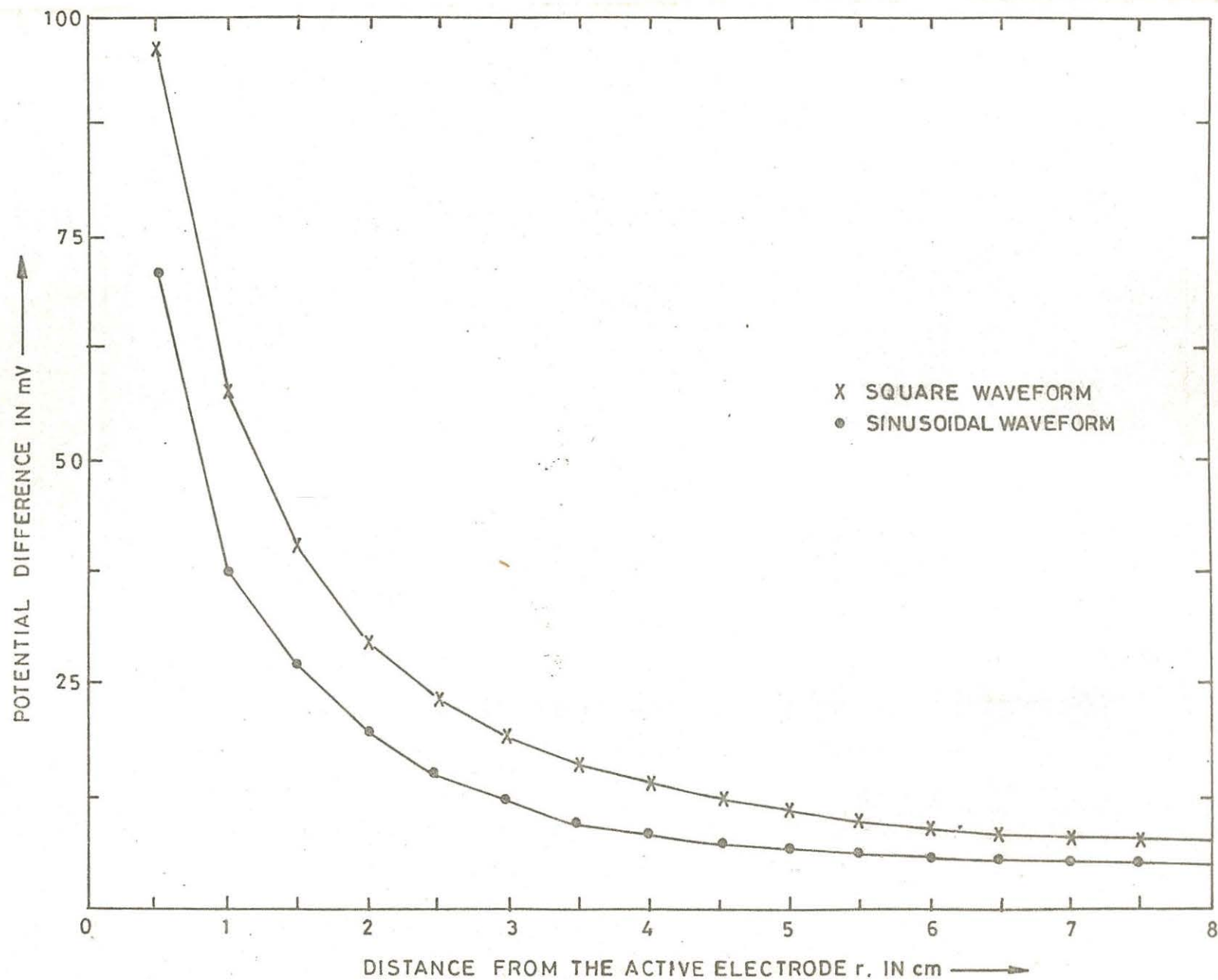


Fig. 6.4 Potential distributions ( $\phi$ ) as a function of distance of the probe from the active electrode ( $r$ ) with stimulation waveform as a parameter during monopolar stimulation.

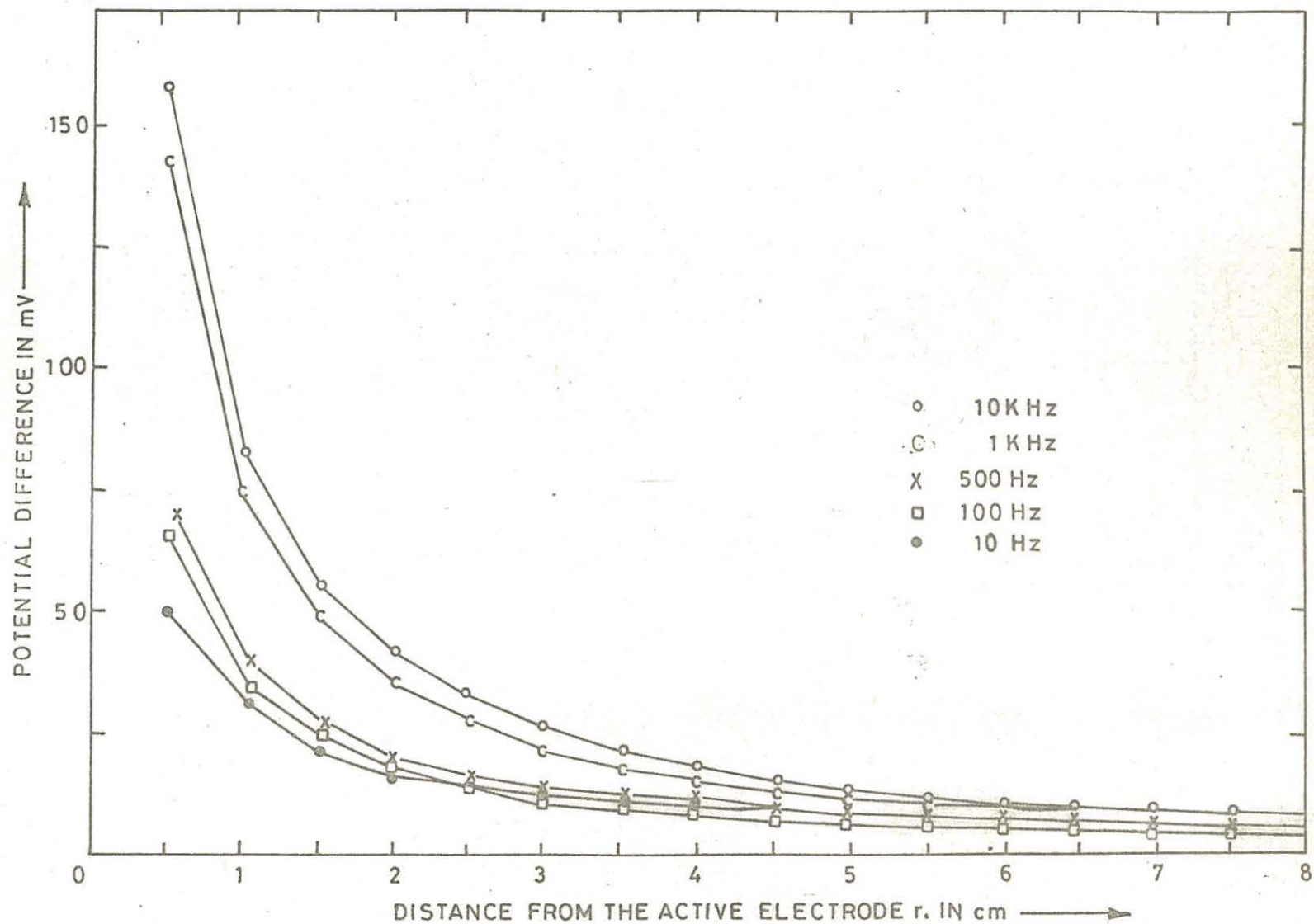


Fig. 6.5 Potential distributions ( $\phi$ ) as a function of distance of the probe from the active electrode ( $r$ ) with stimulation frequency as a parameter during monopolar stimulation.

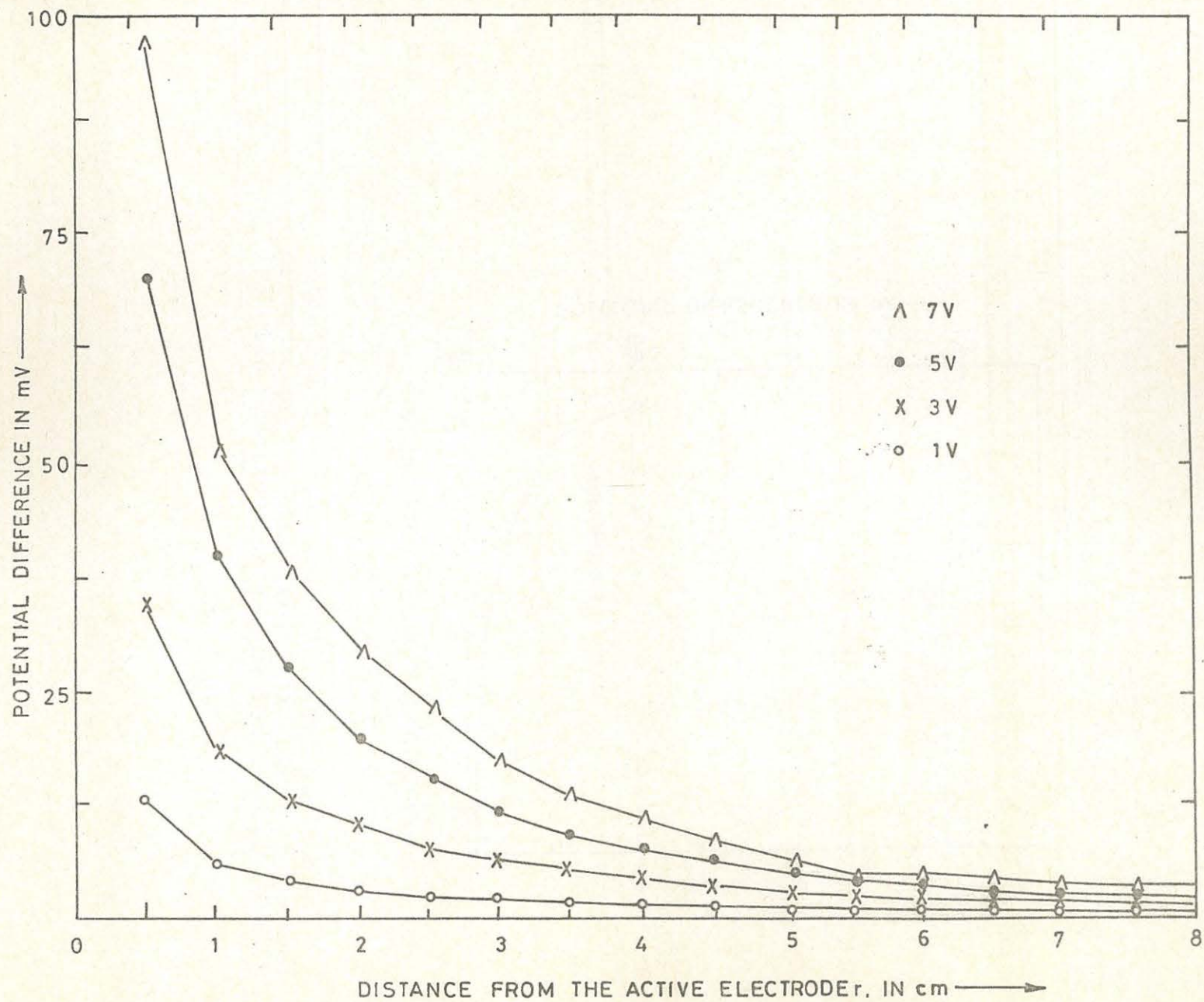


Fig. 6.6 Potential distributions ( $\phi$ ) as a function of distance of the probe from the active electrode ( $r$ ) with stimulation voltage as a parameter during monopolar stimulation.

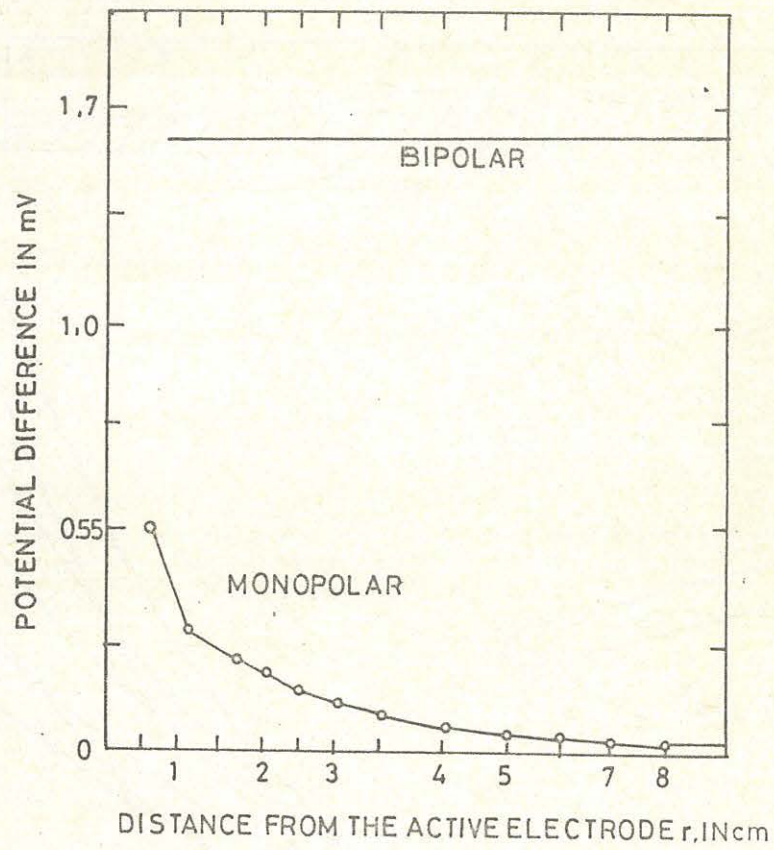


Fig. 6.7 Potential distributions ( $\phi$ ) as a function of distance of the probe from the active electrode ( $r$ ) with electrode configuration as a parameter.

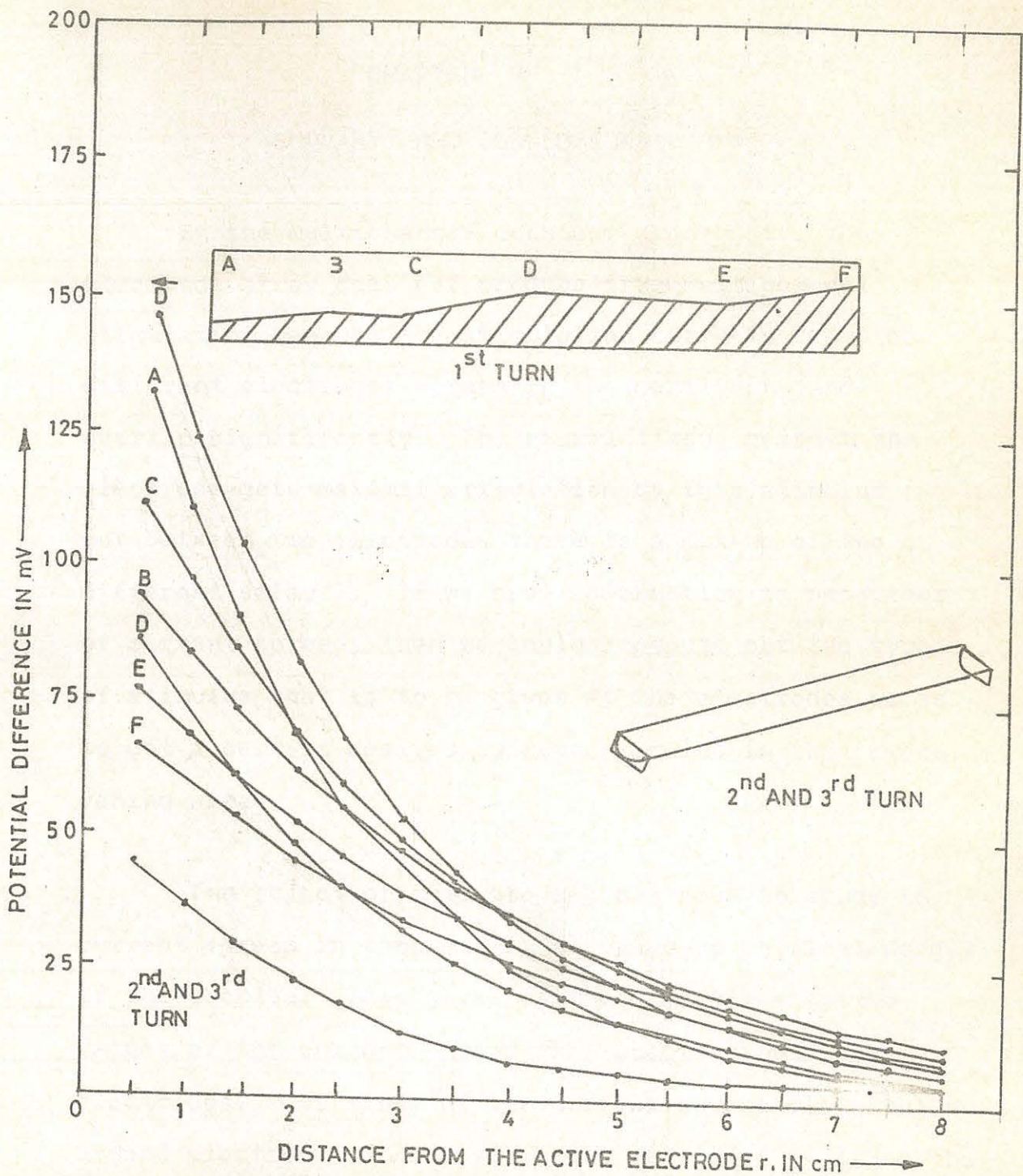


Fig. 6.8 Potential distributions ( $\phi$ ) as a function of distance of the probe from the active electrode ( $r$ ) in scaled-up physical models of the scala tympani during monopolar stimulation.

## CHAPTER 7

## SUMMARY AND CONCLUSIONS

In the multichannel cochlear prosthesis, the electrode array does not produce true multichannel stimulation because the stimulation currents from the different electrodes spread in the perilymph, and overlap significantly. The neural tissue nearest the electrode gets maximal stimulation by this stimulus but between two electrodes there is a mix-up of two different stimuli. If we have information on behaviour of current spread, then we could compute out the type of stimulus that is to be given at the electrodes so as to get a certain desired current stimulus in the intervening areas.

The object of this project has been to study the current spread in tank models & scaled-up physical models of the cochlea. This gives us the directly recorded values of the current spread that occurs around the electrodes. Our study of the current spread distribution around electrodes was based on the method of plotting the potential distribution described by Vagramyan (1961).

The cochlea when stretched out lengthwise, appears like being made by joining two tubes of different geometries. From literature, the correct dimensions of the cochlea was obtained. The sharp angles in the first turn of the scala tympani were calculated. By scaling up the length and radii twenty times its original size, we could maintain the same angulations as that of the scala tympani while the resistance of each segment decreased proportionately by a factor of twenty. With these dimensions it was possible to construct models of the scala tympani, the compartment where the electrodes are implanted in cochlear prostheses.

The potential differences between the active electrode and the probe electrode in the two physical models of the scala tympani have been measured. By using the equation  $J = \sigma \, d\phi / dx$ , we can calculate the current density distribution from the above measurements.

The data obtained from this study may be useful for stimulus deconvolution techniques in cochlear stimulation strategies. A method of finding out the current density distribution pattern in the assymetrical geometry of the scala tympani from the above values of the potential differnnces should be evolved. Computer simulation studies can be done making use of the above

data and the results verified. Further, an attempt can be made to utilise the above results in physiological experiments.

- Baker, C.C. (1989) "Principles of the impedance technique", IEEE Engg in Med & Biol Mag, March, pp 10-15.
- Ballantyne, J.C., Evans, E.F., & Morrosion, A.W. (1978) "Electrical auditory stimulation in the management of the profound hearing loss", J of Laryngology & Otology Suppl, v 26, pp 24-25.
- Ballantyne, J.C. (1988) Scott Brown's Diseases of the Ear, Nose and Throat. v 4, pp 506- 529. London: Butterworths.
- Banfai, P., Hartmann, G., Kubik, S., Darczag, A., Luers, P., & Surth, W. (1985) "Extracochlear eight channel electrode system", J of Laryngology & Otology, v 99, pp 549-53.
- Beagley, H.A. (1979) Auditory Investigation : Scientific & Technological Basis. Oxford: Clarandon.
- Bekesy, G. von (1960) Experiments in Hearing. New York: McGraw Hill.
- Bhargav, K.B. & Shah, T.M. (1987) A Short Textbook of Ear, Nose, and Throat Diseases for Students and Practitioners. Bombay: Usha.
- Birrell, J.F. (1984) Logan Turner's Diseases of Nose, Throat & Ear. Bristol: John Wright.
- Black, R.C. & Clark, G.M. (1980) "Differential electrical excitation of the auditory nerve", J Acoust. Soc. Am., v 67(3), pp 321-323.
- Black, R.C., Clark, G.M., & Patrick, J.F. (1981) "Current distribution measurements within the human cochlea", IEEE Trans BME 28(10), pp 17-19.
- Brackmann, D.E. (1986) The Cochlear Prosthesis. London: Karger.
- Chatterjee, C.C. (1956) Human Physiology. Calcutta: Modern India.
- Clark, G.M., Black, R., Forster, I.C., Patrick, J.F., & Tong, Y.C. (1978) "Design criteria of a multiple-electrode cochlear implant hearing prosthesis", J. Acoust. Soc. Am., v 63, pp 631-32.

- Finley, C.C., Blake, S.W., & White, M.W. (1987), "A finite-element model of bipolar field pattern in the electrically stimulated cochlea - a two dimensional approximation", Proc. IEEE Conf. Engg. Med. Biol. Soc, pp 1901-1902.
- Fravel, R., ed (1986) Cochlear Implants. Otolaryngologic Clinics of North America, v 19(20), pp 217- 431.
- Girzon, G. & Eddington, D.K. (1987) "A three- dimensional electro-anatomical model of the implanted cochlea", Proc. IEEE Conf. Engg. Med. & Biol. Soc., PP 1904-1905.
- Glass, I. (1985) "Responses of cochlear nucleus units to electrical stimulation through a cochlear prosthesis : channel interaction", Hearing Research, v 17(2), pp 115-26.
- Gray, R.F. (1985) Cochlear Implants. London: Croom-Helm.
- Guyton, A.C. (1984), A Textbook of Medical Physiology. London: Saunders.
- House, W.F. (1986), in Cochlear Implants. Otolaryngologic Clinics of North America, v 19(20), p 217.
- Kauffman, C. & Achilles, A. (1987) "Potentials around electrode tips with implications for cochlear implants", Annals Otol. Rhinol. & Laryngol, v 96, pp 21-22.
- Kiang, N.Y.S. & Moxon, E.C. (1972), "Physiological considerations in artificial stimulation of the inner ear", Annals Otol. Rhinol. & Laryngol., v 81, pp 714-730.
- Kiedel, W.E. (1979), "Neurophysiological requirements for implanted cochlear prostheses", Acta Oto-Laryngol., v 87, pp 163-64.
- Kiedel, W.E. & Finkenzeller, P., eds., (1984) Advances in Audiology, v I & II. London: Karger.
- Kortum, G. (1961) Treatise on Electrochemistry. London: Elsevier.
- Kubasov, V., & Zaretsky, S. (1987) Introduction to Electrochemistry. Moscow: Mir
- Lukies, P.M., Tong, Y.C. & Clark, G.M. (1987) "Current distributions produced by the banded electrode array: an experimental study conducted with a tank model", Annals

Otology, Rhinology & Laryngology, v 96, pp 24-25.

Muhamud, M. (1984) A Short Textbook of Ear, Nose & Throat Diseases. New Delhi: Jaypee.

O'leary, S.J., Black, R.C., & Clark, G.M. (1985), "Current distributions in the cat cochlea : a modelling and electrophysiological study", Hearing Research, v 18(3), pp 130.

Pandey, P.C. (1987) Speech Processing for Cochlear Prosthesis, Ph.D. thesis, Department of Electrical Engineering, University of Toronto, Canada.

Peter, S. (1970) Biophysical Measurements. Beaverton: Techtronix.

Pickett, J.M. & Levitt, H. (1972) "Electrical stimulation of hearing", J. Acoust. Soc. Am., v 52, pp 694-695.

Pickett, D.J. (1979) Electrochemical Reactor Design. London: Elsevier.

Pracy, R., Siegler, J. & Stell, P.M. (1983) A Short Textbook of Ear, Nose & Throat Diseases. London: English Language Book Society.

Rubinstein, J.T., Susserman, M., & Spelman, F.A. (1987) "Measurements and models of potential fields above recessed electrodes". Proc. IEEE Conf. Engg. Med. Biol. Soc., pp 1903-1904.

Simmons, F.B. (1964), "Electrical stimulation of the auditory nerves and inferior colliculus in man", Arch Otolargol., v 79, pp 559-563.

Tonndorf, J. (1986) Audiology & Audiological Medicine. London: Varges.

Tong, Y.C. & Clark, G.M. (1985), "Absolute identification of electric pulse rates and electrode positions by cochlear implant patients", J Acoust. Soc. Am. v 77(5), pp 1881-1888

Tortora, Y. & Anagnostakos, K. (1988) Principles of Anatomy & Physiology. London: Harper & Row.

Vagramyan, T. & Solov'ena, G. (1961) Principles of Electrochemistry. London: Elsevier.

White, R.L. & Von Compernelle, D. (1987) "Current spreading and speech processing strategies for cochlear prosthesis", Annals Otol. Rhinol. Laryngol., v 96, pp 22-25.

Zemlin, G.Y. (1985) Anatomy & Physiology of Speech & Hearing Science. London: Saunders.